NASA Contractor Report 195295

Real-Time Sensor Data Validation

Timothy W. Bickmore
GenCorp
Aerojet Propulsion Division
Sacramento, California

April 1994

Prepared for
Lewis Research Center
Under Contract NAS3–25883

National Aeronautics and
Space Administration

Real-Time Sensor Data Validation

October 1, 1993

Development of Life Prediction Capabilities
for Liquid Propulsion Rocket Engines Program

Contract Number: NAS 3-25883

T.W. Bickmore

Contents

Summary 1
I. Introduction 2
II. Program Status 2
II.1. System Architecture Study 2
II.2. Probabilistic Approach to Analytical Redundancy 3
II.3. Empirical and Characteristic Modeling 15
II.4. Summary of Work to Date 31
III. Guidelines for the Development of SDV Models 32
III.1. Sensor vs. Plant Anomaly Discrimination 32
III.2. Statistical Independence of Sensor Failures 33
III.3. Adapting Models to New LRUs 33
III.4. Summary 34
IV. FY93–95 Task Description 35
IV.1. Scope 35
IV.2. Hard Failure Detection in Redline Sensors 35
IV.3. Operation During Power-Level Transients 35
IV.4. Operation During START Transient 35
IV.5. Integration of Advanced Models 36
IV.6. Software Development and Test 37
V.FY93–95 Programmatics 38
V.1. Expanded Work Breakdown Structure 38
V.2. Schedule & Milestones 43
References 45
Attachment 1—Empirical Models Selected for FY92 Modeling Task 47
Attachment 2—Empirical Model Coefficients Averaged Over Training Datasets 57
Attachment 3—Characteristic Equation Coefficients Derived in FY 92 Modeling Task 65

Nomenclature

APD	Aerojet Propulsion Division
AREC	Aerojet's Advanced Rocket Engine Controller
CADS	Command and Data Simulator
FPB	Fuel Preburner
HPFP	High Pressure Fuel Pump
HPFT	High Pressure Fuel Turbine
HPOP	High Pressure Oxidizer Pump
HPOT	High Pressure Oxidizer Turbine
JSC	Johnson Space Center
LeRC	Lewis Research Center
LOX	Liquid Oxygen
MCC	Main Combustion Chamber
MSFC	Marshall Space Flight Center
MTBF	Mean Time Between Failure
PID	Parameter ID (Sensor Identification Number)
PBP	Preburner Boost Pump
PC	Chamber Pressure
SDV	Sensor Data Validation
SSC	Stennis Space Center
SSME	Space Shuttle Main Engine
TTB	Technology Test Bed
TTBE	Technology Test Bed Engine

Summary

This report describes the status of an on-going effort by the NASA Lewis Research Center and Aerojet Propulsion Division to develop software capable of detecting sensor failures on liquid rocket engines in real time, and with a high degree of confidence. This software could be used in a rocket engine controller to prevent the erroneous shutdown of an engine due to sensor failures which would otherwise be interpreted as engine failures by the control software.

The approach taken combines analytic redundancy with Bayesian belief networks to provide a solution which has well-defined real-time characteristics, well-defined error rates, and is scaleable to validate any number of engine sensors. Analytical redundancy is a technique in which a sensor's value is predicted by using values from other, usually non-redundant, sensors and known or empirically derived mathematical relations. For example, given the engine plant diagram in Figure 1, fuel flow can be related to either the low pressure pump speed or the high pressure pump speed by a pump affinity equation (assuming constant fuel density). As shown, a set of sensors and a set relationships among them form a network of cross-checks which can be used to periodically validate all of the sensors in the network. Bayesian belief networks provide a mathematically sound method of determining if each of the sensors in the network is valid, given the results of all of these cross-checks.

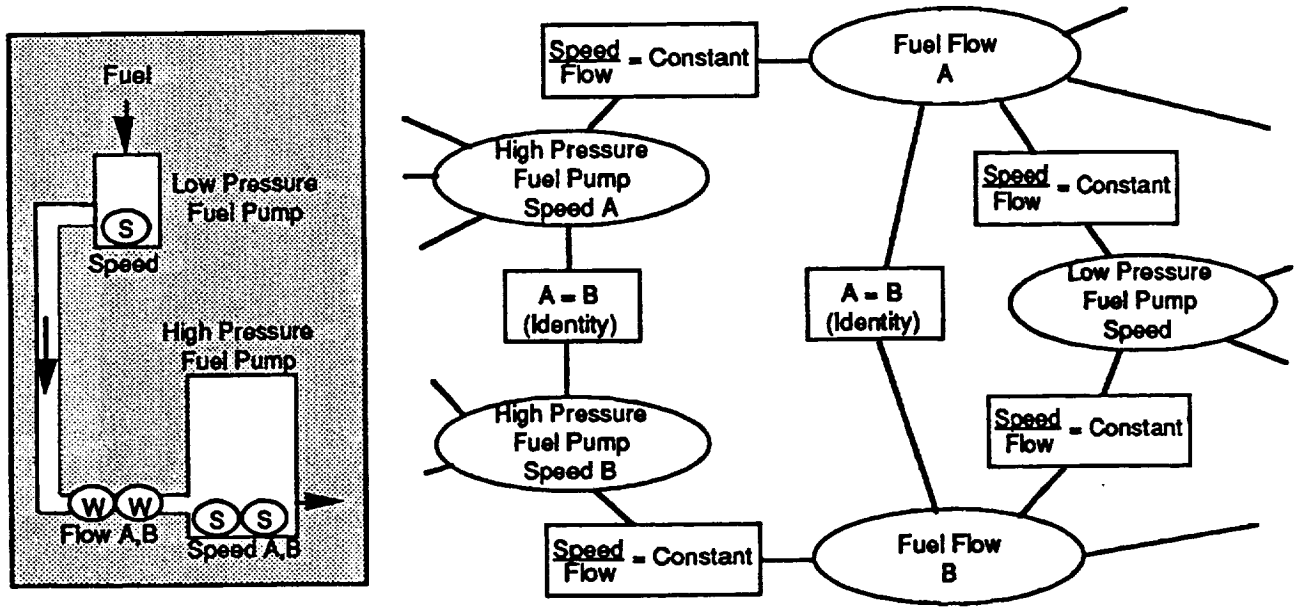

Figure 1. Example Engine Plant Diagram and Partial Sensor Validation Network

This approach has been codified in an algorithm which has been successfully demonstrated on a rocket engine controller in real-time on the Technology Test Bed Engine at the NASA Marshall Space Flight Center. Current efforts are focused on extending the demonstration system to provide a real-time validation capability for approximately 100 sensors on the Space Shuttle Main Engine.

I. Introduction

The safety and reliability of rocket engines would be enhanced if engine controllers and advanced safety systems could determine if sensors were supplying faulty data. This ability, termed sensor data validation, could prevent the controller or safety system from making critical decisions, such as the decision to shut an engine down, on the basis of data from anomalous or failed sensors.

An approach to validating sensors in real-time has been developed and demonstrated on the Technology Test Bed Engine (TTBE) at the NASA Marshall Space Flight Center (MSFC). The demonstration system validated six channels of sensor data in real-time, running on a state-of-the-art engine controller.

The current effort involves extending the demonstration system in the following ways:

- The number of sensors validated will be increased from six to approximately 97.
- The system will monitor continuously during mainstage (the first demonstration system only operated during steady-state intervals).
- Hard failures in control and redline sensors will be detected before the engine controller responds.
- As an option, the system will monitor control and redline sensors during the engine startup transient.

The extended system will be implemented on a 486PC in the Technology Test Bed (TTB) blockhouse which receives data in real-time during TTBE firings. The completed system will be validated on at least 20 engine firings.

This report describes the status of an on-going effort by the NASA Lewis Research Center (LeRC) and Aerojet Propulsion Division (APD) to develop a software solution to the sensor data validation problem capable of running in a ground test computer or rocket engine controller. A program plan is then presented in detail for continuation of this work by Aerojet in FY93-FY95 on the Real-Time Sensor Data Validation task of the Development of Life Prediction Capabilities for Liquid Propulsion Rocket Engines contract. This project is being funded by the NASA OACT ETO program.

II. Program Status

Efforts to develop an approach to real-time sensor data validation (SDV) for liquid rocket engines have evolved over four years (see Figure 2), from conceptual design (FY90) to software implementation and test in a rocket engine controller on the TTB test stand (FY92). More recent efforts have focused on scaling up the capability demonstrated on TTB to validate the majority of control and health monitoring sensors on the Space Shuttle Main Engine (SSME).

II.1. System Architecture Study

In FY90 a System Architecture Study of SDV was performed by Aerojet which reviewed common sensor failure modes on the SSME, the data validation process used by SSME data analysts at MSFC, and a number of alternative approaches to automating SDV for post-test/post-flight data analysis.[1]

The approaches to SDV reviewed included range and rate limit checking[2,3], various pattern-matching techniques[4-9], and analytical redundancy[10-12]. The conclusion of this study was that no single algorithmic method should be used for SDV; rather several methods should be used to analyze sensor data and the results integrated or "fused" into a final conclusion regarding the integrity of each sensor. Several approaches to information fusion were also reviewed for their applicability to SDV, including binary logic, ad-hoc

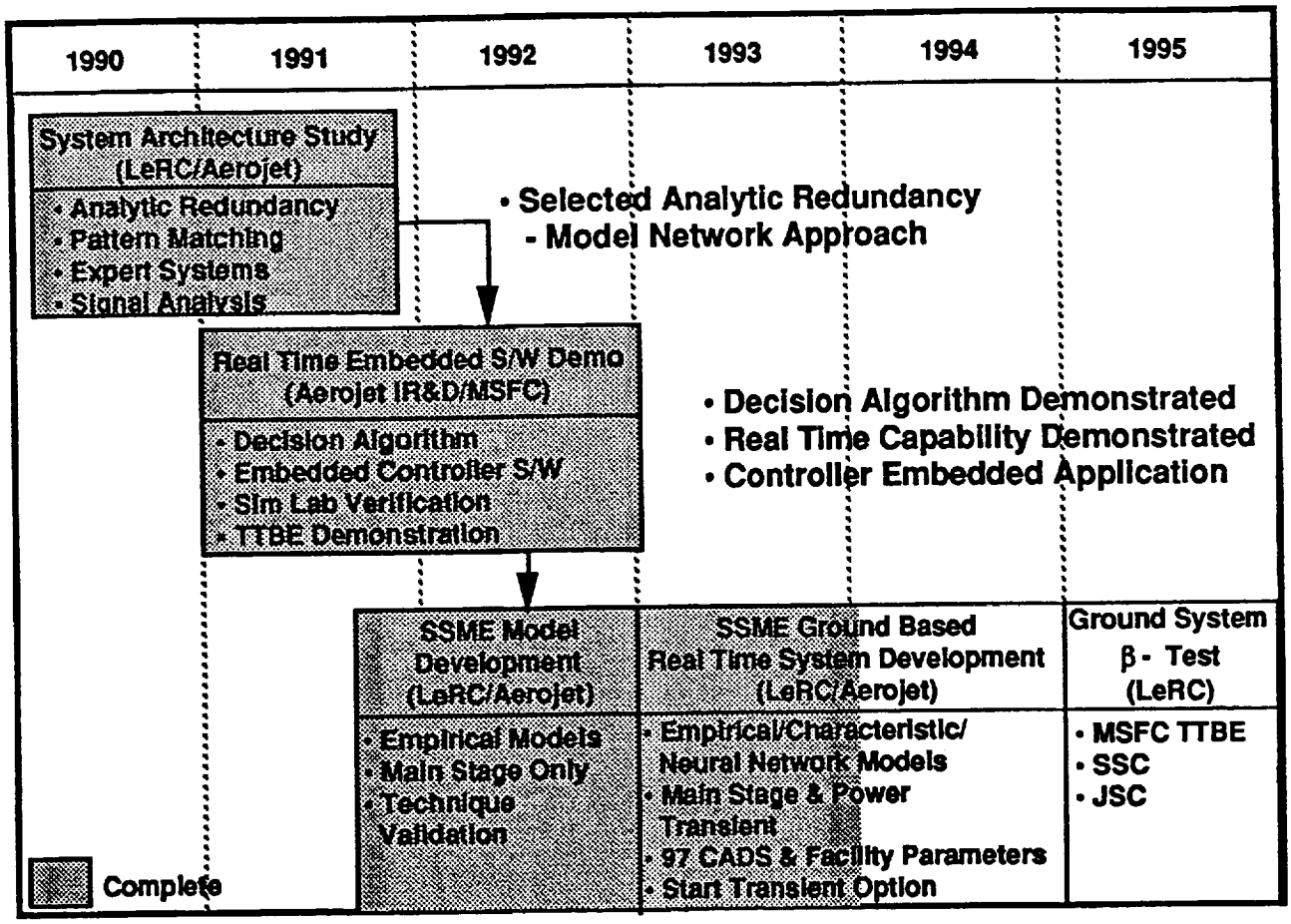

Figure 2. Real-Time Sensor Data Validation Program History

certainty factors[13], Dempster-Shafer theory[14], and Bayesian belief networks[15]. Bayesian belief networks were selected as the best strategy, since they were believed to be the most mathematically sound approach to information fusion.

II.2. Probabilistic Approach to Analytical Redundancy

Real-time sensor data validation was targeted as a demonstration application for APD's Advanced Rocket Engine Controller (AREC), developed on APD's Integrated Controls and Health Management IR&D in FY91 (Project AMP91-03). The approach taken combined analytical redundancy with Bayesian information fusion techniques to achieve a solution which has well-understood false alarm and missed detection error rates, operates within hard time constraints, and is scaleable to validate any number of sensors.[16]

Analytical redundancy is a technique in which a sensor's value is predicted by using values from other, usually non-redundant, sensors and known or empirically derived relations among the sensor values. For example, Figure 3 shows a relation among three sensor values using a standard formula for fluid line resistance. Relations can also be empirically derived using standard statistical regression techniques. The simplest form of these empirical relations is a linear equation relating two sensor values, as shown in Figure 4. In general, a relation is used to provide validation information for all related sensors.

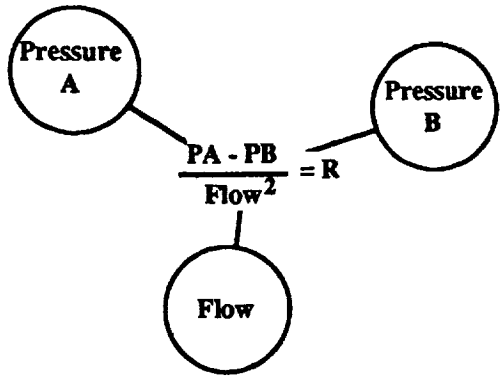

Figure 3. Example Characteristic Relation

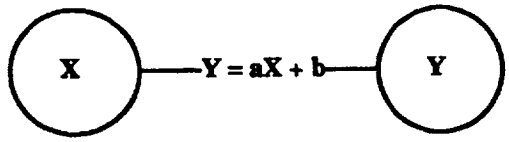

Figure 4. Example Statistical Relation

A group of sensors and a set of relations among them define a network. Figure 5 shows a very simple example of a sensor validation network for three parameters on the SSME.

The difference between a value predicted using a relation and a directly sensed value is called a *residual,* and is a measure of the quality of the relation, given that the sensors involved are known to be working properly. In the approach taken in this work, one or more algebraic relations are defined for every sensor in the network which relate its value to the values of one or more other sensors in the network. The mean and standard deviation of the relation residuals (evaluated on normal engine test firing data) are also computed.

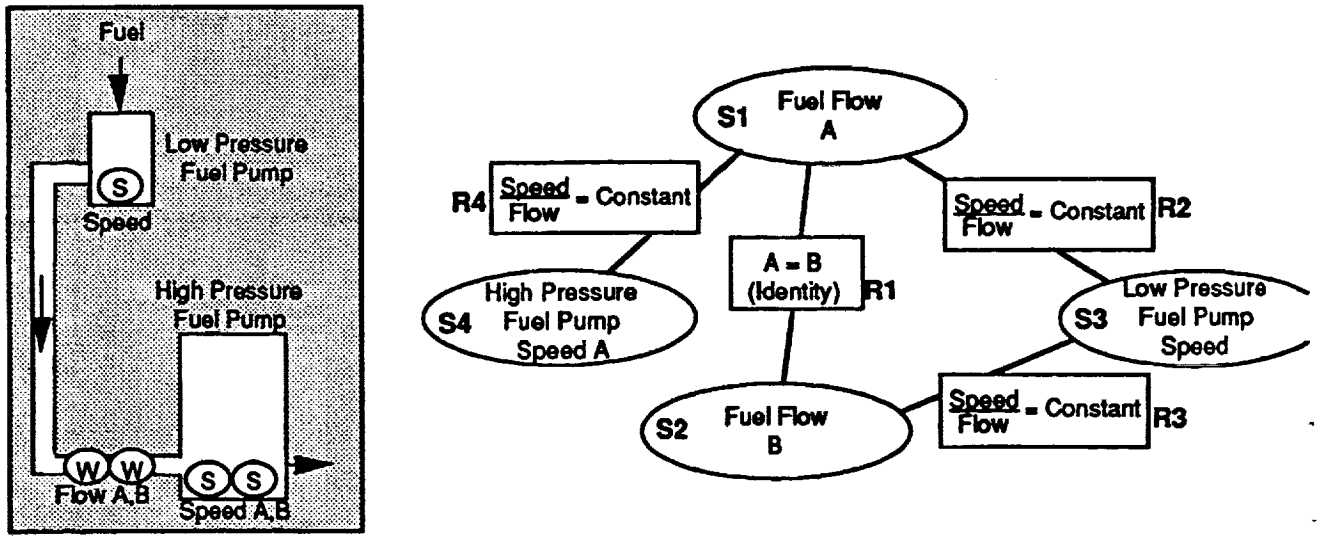

Figure 5. Example Sensor Validation Network

Given this information, a validation algorithm could sample sensor values every controller cycle during an engine firing and determine if each of the relations holds or not by thresholding on a particular residual, such as three standard deviations. Once the status of every relation in the network has been determined to either "hold" or "not hold", the validation algorithm makes a conclusion about the validity of each sensor in the network (the one-cycle decision problem). Conclusions made during several consecutive controller cycles may be fused together in order to disqualify a sensor (the multi-cycle decision problem). Figure 6 summarizes this overall approach.

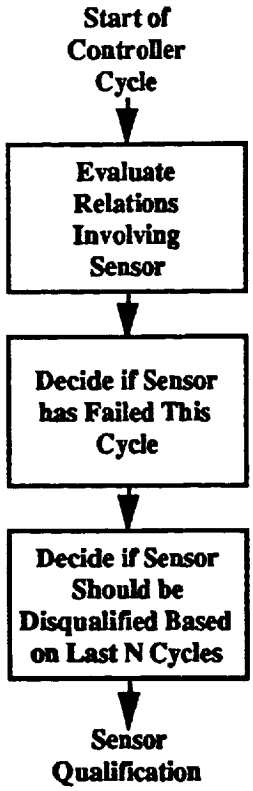

Figure 6. Overall Approach to Real-Time Sensor Data Validation

Before this general approach could be implemented, several questions needed to be answered:

- How many relations are needed to validate a sensor?
- How many of a sensor's relations need to hold in order to validate the sensor during one controller cycle?
- What threshold should be used on the individual relation residual tests?
- Should sensor value averaging or other multi-cycle strategies be used?
- Can a scaleable approach to validation be developed which will work with any number of sensors?
- Do all relations need to be evaluated every cycle to validate all sensors?

Bayesian Analysis

Bayesian probability theory provides a formal framework within which the questions posed above can be answered. Bayesian probability theory provides a mathematically sound approach to the problem of *information fusion* — the combination of evidence from

several sources into a single, consistent model. In information fusion, uncertainties in the sources of evidence (i.e., inaccuracies in the sensors or uncertainties in the fault detection algorithms themselves) are explicitly modeled and accounted for.

A Bayesian Belief Network is a graphical representation of a joint probability distribution of a set of random variables.[15,17,18] As an example, the validation network shown in Figure 5 can be represented as the Belief Network shown in Figure 7. In this network, the nodes S1, S2, and S3 represent the status of the respective sensors (i.e. whether they are working or not), while the nodes R1, R2, and R3 represent whether an analytical redundancy relationship currently holds between the sensors or not. Connections in the network represent influences between variables. In Figure 5, for example, a failure in sensor S1 would influence the expected probability distribution on the status of relation R1.

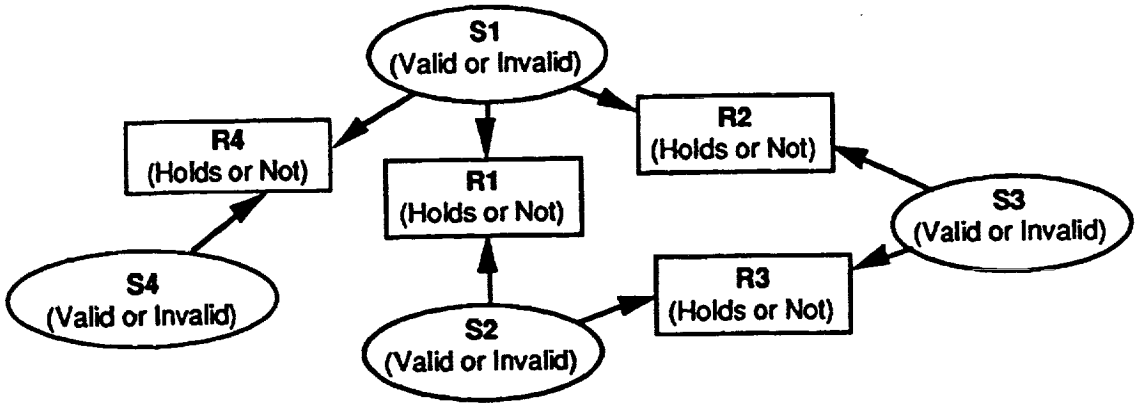

Figure 7. Example Sensor Validation Network Cast into a Bayesian Belief Network for Analysis

Given the Belief Network shown in Figure 7, the probability of each sensor being valid given the current status of all relations can be derived. These equations can then be used to answer the questions posed above, and to develop a mathematically sound approach to sensor data validation.

The following assumptions were made in the FY91 activity in order to conduct the Bayesian analysis:

- Although several sensors may fail during a firing, two sensors cannot fail during a single controller cycle. The likelihood of two or more sensors initiating a failure at the same instant in time is very remote, and it would greatly complicate the validation system to accommodate such simultaneous multiple-point failures.
- Once a sensor is determined to have failed, it will stay failed and will not be used again in any future calculations.
- The reliability of a sensor can be determined from its Mean Time Between Failure (MTBF). This measure is assumed to be constant for the duration of a single engine firing.
- When a sensor fails it emits random values. This is a very conservative assumption, and is a more difficult failure mode to detect than a hard failure (i.e., if the algorithm is able detect the random failure mode with a high degree of confidence, it will also be able to detect hard and drift failures). This is an admission that a failed sensor has

some small probability of emitting a value which is within the realm of "reasonableness" for the parameter being measured.

The conditional probabilities required to fully define the Belief Network shown in Figure 7 were derived from the assumptions given above. The following derivations assume that all relations are binary (i.e., integrate information from two sensors).

The probability of a sensor failing on a particular controller cycle is given by

Equation 1. $P(\text{Sensor Invalid}) = \text{CycleTime} / \text{MTBF}.$*

Thus, the probability of a sensor with a MTBF of 30 minutes failing during a 40ms sample is 0.0000222, while for a sensor with a MTBF of 20 hours this probability is 0.0000006.

The probability of a relation holding, given that all of the related sensors are working, is determined by the threshold level placed on the relation. Thus,

Equation 2. $P(\text{RelationHolds} \mid \text{Sensor}_1\text{Valid}, \text{Sensor}_2\text{Valid}) = K$

where K is a quantile of the normal distribution (e.g., for a 3 standard deviation relation threshold, K = 0.997).

Since a failed sensor emits random values, there is still some probability, P_n, that a given reading may fall within the normal range of values for the sensor, causing the relation to continue to hold. (Note that for hard sensor failures $P_n = 0$.) If this normal range is taken to be 3 standard deviations, then

Equation 3. $$P_n = \frac{2 \times 3 \times \text{Standard Deviation}}{\text{Range of Sensor}}$$

For SSME sensors, Pn has been empirically determined to be have an average value of 0.22 (although it is slightly different for each sensor). The probability of a binary relation holding given that one of its sensors has failed is thus

Equation 4. $P(\text{RelationHolds} \mid \text{Sensor}_1\text{Invalid}, \text{Sensor}_2\text{Valid}) = P_n$

Equation 5. $P(\text{RelationHolds} \mid \text{Sensor}_1\text{Valid}, \text{Sensor}_2\text{Invalid}) = P_n$

Similarly, the probability of a binary relation holding given that both of its sensors have failed is

Equation 6. $P(\text{RelationHolds} \mid \text{Sensor}_1\text{Invalid}, \text{Sensor}_2\text{Invalid}) = P_n \times P_n$

The probabilities given above yield the following joint probability distribution for the network shown in Figure 7.

Equation 7.
$$P(S1,S2,S3,S4,R1,R2,R3,R4) = P(S1) \times P(S2) \times P(S3) \times P(S4) \times P(R1|S1,S2) \times P(R2|S1,S3) \times P(R3|S2,S3) \times P(R4|S1,S4)$$

* "P(A)" can be read as "the probability of A being true". "P(A,B)" can be read as the "the probability of A and B being true." "P(A | B)" can be read as "the probability of A being true given that B is true". "P(A | B,C)" can be read as the "the probability of A being true given that B and C are true".

Given the joint distribution, the goal is to determine the probability of any one sensor working given the status of all relations in the network (this is the basis for the real-time, one-cycle decision problem). This can be achieved by using Bayes' rule. For example, after measurements for S1, S2, S3, and S4 have been taken, and relations R1, R2, R3, and R4 have been evaluated to determine whether they hold or not, the probability of sensor S1 working can be determined as follows.

Equation 9. $$P(S1|R1,R2,R3,R4) = \frac{P(S1,R1,R2,R3,R4)}{P(R1,R2,R3,R4)}$$ *Baye's Rule*

Where,

Equation 10.

$$\begin{aligned} P(S1,R1,R2,R3,R4) = \\ P(S1,S2=Valid,S3=Valid,S4=Valid,R1,R2,R3,R4) + \\ P(S1,S2=Valid,S3=Invalid,S4=Valid,R1,R2,R3,R4) + \\ P(S1,S2=Invalid,S3=Valid,S4=Valid,R1,R2,R3,R4) + \\ P(S1,S2=Invalid,S3=Invalid,S4=Valid,R1,R2,R3,R4) + \\ P(S1,S2=Valid,S3=Valid,S4=Invalid,R1,R2,R3,R4) + \\ P(S1,S2=Valid,S3=Invalid,S4=Invalid,R1,R2,R3,R4) + \\ P(S1,S2=Invalid,S3=Valid,S4=Invalid,R1,R2,R3,R4) + \\ P(S1,S2=Invalid,S3=Invalid,S4=Invalid,R1,R2,R3,R4) \end{aligned}$$

and

Equation 11.

$$\begin{aligned} P(R1,R2,R3,R4) = \\ P(S1=Valid,S2=Valid,S3=Valid,S4=Valid,R1,R2,R3,R4) + \\ P(S1=Valid,S2=Valid,S3=Invalid,S4=Valid,R1,R2,R3,R4) + \\ P(S1=Valid,S2=Invalid,S3=Valid,S4=Valid,R1,R2,R3,R4) + \\ P(S1=Valid,S2=Invalid,S3=Invalid,S4=Valid,R1,R2,R3,R4) + \\ P(S1=Invalid,S2=Valid,S3=Valid,S4=Valid,R1,R2,R3,R4) + \\ P(S1=Invalid,S2=Valid,S3=Invalid,S4=Valid,R1,R2,R3,R4) + \\ P(S1=Invalid,S2=Invalid,S3=Valid,S4=Valid,R1,R2,R3,R4) + \\ P(S1=Invalid,S2=Invalid,S3=Invalid,S4=Valid,R1,R2,R3,R4) + \\ P(S1=Valid,S2=Valid,S3=Valid,S4=Invalid,R1,R2,R3,R4) + \\ P(S1=Valid,S2=Valid,S3=Invalid,S4=Invalid,R1,R2,R3,R4) + \\ P(S1=Valid,S2=Invalid,S3=Valid,S4=Invalid,R1,R2,R3,R4) + \\ P(S1=Valid,S2=Invalid,S3=Invalid,S4=Invalid,R1,R2,R3,R4) + \\ P(S1=Invalid,S2=Valid,S3=Valid,S4=Invalid,R1,R2,R3,R4) + \\ P(S1=Invalid,S2=Valid,S3=Invalid,S4=Invalid,R1,R2,R3,R4) + \\ P(S1=Invalid,S2=Invalid,S3=Valid,S4=Invalid,R1,R2,R3,R4) + \\ P(S1=Invalid,S2=Invalid,S3=Invalid,S4=Invalid,R1,R2,R3,R4) \end{aligned}$$

Each term of these latter two equations can be evaluated using the joint probability distribution given in Equation 7.

Given the ability to compute the probability of a sensor being valid or not given the status of all relations in the network (as in Equation 9), an optimum one-cycle decision strategy can be developed by simply thresholding on this probability. Table 1 shows the validation probabilities for sensor S1 given that the MTBF of S1, S2, S3, and S4 in Figure 7 is 30 minutes, the relation residual threshold for R1, R2, R3, and R4 is 3 standard deviations, and P_n is 0.22. From this table it can be seen that the optimum strategy, given these assumptions, is to disqualify sensor S1 when relations R1, R2, and R4 do not hold.

P(S1=Valid|R1=Holds,R2=Holds,R3=Holds,R4=Holds)	= 1
P(S1=Valid|R1=Holds,R2=Holds,R3=Holds,R4=NotHold)	= 0.9997204
P(S1=Valid|R1=Holds,R2=Holds,R3=NotHold,R4=Holds)	= 1
P(S1=Valid|R1=Holds,R2=Holds,R3=NotHold,R4=NotHold)	= 0.9997204
P(S1=Valid|R1=Holds,R2=NotHold,R3=Holds,R4=Holds)	= 0.9997191
P(S1=Valid|R1=Holds,R2=NotHold,R3=Holds,R4=NotHold)	= 0.7523449
P(S1=Valid|R1=Holds,R2=NotHold,R3=NotHold,R4=Holds)	= 0.9998867
P(S1=Valid|R1=Holds,R2=NotHold,R3=NotHold,R4=NotHold)	= 0.8828096
P(S1=Valid|R1=NotHold,R2=Holds,R3=Holds,R4=Holds)	= 0.9997191
P(S1=Valid|R1=NotHold,R2=Holds,R3=Holds,R4=NotHold)	= 0.7523449
P(S1=Valid|R1=NotHold,R2=Holds,R3=NotHold,R4=Holds)	= 0.9998867
P(S1=Valid|R1=NotHold,R2=Holds,R3=NotHold,R4=NotHold)	= 0.8828096
P(S1=Valid|R1=NotHold,R2=NotHold,R3=Holds,R4=Holds)	= 0.7515119
P(S1=Valid|R1=NotHold,R2=NotHold,R3=Holds,R4=NotHold)	= 0.002574868
P(S1=Valid|R1=NotHold,R2=NotHold,R3=NotHold,R4=Holds)	= 0.9227433
P(S1=Valid|R1=NotHold,R2=NotHold,R3=NotHold,R4=NotHold)	= 0.01009216

Table 1. Example Validation Probabilities for Sensor S1

There are two measures of quality for any validation algorithm; the false alarm and missed detection rates (equivalent to Type I and Type II errors in statistics, respectively[19]). The false alarm rate is the probability that the validation system will disqualify a sensor, when it is in fact working correctly. The missed detection rate is the probability that the validation system will qualify a sensor, when it has in fact failed (this is related to the notion of sensitivity). These rates can be computed for the one-cycle decision strategy described above. The false alarm rate for sensor S1 is the sum of

$$P(S1=Valid,S2,S3,S4,R1,R2,R3,R4)$$

in all situations in which the validation system decides to disqualify S1. For the example given above, the false alarm rate is

$$\begin{array}{r} 2.71412E\text{-}8 \\ +\ \underline{3.27073E\text{-}10} \\ 2.74683E\text{-}8 \end{array}$$

Similarly, the missed detection rate for sensor S1 is the sum of

$$P(S1=Invalid,S2,S3,S4,R1,R2,R3,R4)$$

in all situations in which the validation system decides to validate S1. For the example given above, the missed detection rate is 1.16765E-5.

These two quality measures were used to evaluate many alternative answers to the questions posed above. The results indicated that:

- At least three relations involving a sensor's value are required to provide enough information to disqualify the sensor.
- The number of relations involving a sensor's value which must be violated in order to disqualify the sensor varies with the number of relations. For example, in the network

shown in Figure 7 in which sensor S1 is involved in three relations, all three relations must be found not to hold before the common sensor can be disqualified.

- A 3 standard deviation residual threshold should be used on all relations to determine if they hold or not.
- A multi-cycle decision strategy must be used in order to get the error rates below acceptable levels. The best strategy evaluated was a 3-of-5 strategy, in which a sensor must be judged bad (using the one-cycle strategy) on at least three of the last five controller cycles before it can be conclusively disqualified.

Of the results obtained, the most significant was that only the relations directly bearing on a sensor need to be evaluated in order to validate the sensor. For example, in the network shown in Figure 7 only relations R1, R2, and R4 need to be considered when validating S1 (see Table 1).

Given this, and the fact that a voting table can be constructed which specifies the number of those relations which must be violated before the sensor can be disqualified, an algorithm can be designed which only evaluates relations for a particular sensor until it is impossible to disqualify it. For example, when validating sensor S1 in the network shown in Figure 7, the relations R1, R2, and R4 can be examined in sequence, but as soon as one is found to hold, the validation process for S1 can stop because it is impossible to disqualify it (i.e., all three relations must be violated in order to disqualify a sensor with three relations). Thus, all relations in the network do not need to be evaluated every cycle.

The maximum number of relations which can be expected to fail per controller cycle can be computed and translated into a hard upper bound on processing time for the validation system. Assuming that at most one sensor can fail on a given controller cycle, the maximum number of relations which need to be evaluated each cycle is given by the following:

- For each of the valid sensors, the first relation always needs to be evaluated (assuming a 3-of-3 disqualification strategy). However, we can compute the probability of a given number of additional relations failing and pick the smallest number that gives us the reliability we want. The probability of more than r relations out of the total R relations in the network failing (due to noise and modelling errors) is:

$$\sum_{i=r+1}^{R} \binom{R}{R-i} \times P(\text{RelationHolds})^{R-i} \times P(\text{RelationNotHold})^{i}$$

  This is a sum of binomial probabilities, which for large R and small P(RelationNotHold) can be approximated by a sum of Poisson probabilities, with μ=R x P(RelationNotHold). If there are three unique relations for each of 115 sensors on the SSME, then R=115*(3-1)-2=228 and P(RelationNotHold)=0.003 (for a 3-standard-deviation threshold), making μ=0.684. A table of Poisson probability sums[19] indicates that at most nine additional relations would need to be checked to yield a very high degree of confidence.

- Assuming that one sensor did fail on a given cycle, the number of relations that need to be evaluated to confirm the failure is simply the number of immediate relations that the sensor has (in the worst case they would all need to be checked). For a sensor with five relations, all five may need to be evaluated in order to disqualify the sensor.

Thus, for the 114 valid sensors, one relation must always be checked, and we will allow an additional nine to be checked in the overall network to guarantee a high level of confidence. For the one failed sensor, all three of its relations must be checked. Thus, in the worst case, a total of 114 + 9 + 3 = 126 relations need to be evaluated on any given cycle. The small number of relations which need to be evaluated each cycle, coupled with the fact that only the relations directly involving a sensor need to be evaluated for validation, allowed an algorithm to be developed which is entirely scaleable (i.e., will work with a large number of sensors and relations).

These results are based on our assumptions about the accuracy and reliability of the sensors on the SSME. Although studies have shown that these results are insensitive to small changes in the assumed parameter values (corroborated by De Bruyne[20]), large changes would require a new analysis (e.g., if the system were to be used to validate sensors on a power plant). In particular, order-of-magnitude changes in sensor reliabilities would require a re-analysis. Changes in the validation network topology in response to changes in SSME hardware configuration will have no effect on these results.

Software Design, Development and Test

The algorithm and data structures for the core sensor validation routine which performs the one-cycle decision making are outlined in Figure 8 and Figure 9, respectively. Every controller cycle, each sensor is checked in sequence. A sensor check consists of evaluating all of the relations which directly bear on the sensor until a conclusion about its validity can be made. Typically, this will involve evaluating a very small number of relations and then stopping when it becomes impossible to disqualify the sensor. When a sensor is permanently disqualified, all relations which use its value are deactivated. This ensures that the system will not try to perform validation using data from a failed sensor. Thus, the algorithm keeps track of which relations are active and which are inactive, and will continue to validate a sensor even when fewer relations are available.

Several additional software modules were developed to augment the core one-cycle validation routine. These include:

- Steady-State Detection — Detects when the engine has reached one of a known set of steady-state conditions.

```
OneCycleValidate(Sensor)
  Passed ← 0
  Validated ← False
  NumActiveRelations ←
     CountActiveRelations(Sensor.Relation_List)
  DO for each Relation in Sensor.Relation_List UNTIL Validated
    IF(Relation.Status is Active) THEN
          IF(Relation.Eval_Function()) THEN
                Passed ← Passed + 1
                IF(Passed ≥ PassTable[NumActiveRelations]) THEN
                      Validated ← True
  RETURN(Validated)
```

Figure 8. One-Cycle Sensor Validation Algorithm

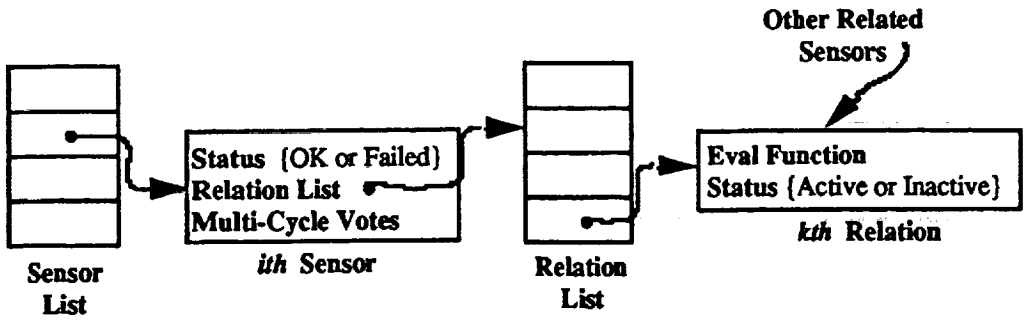

Figure 9. Primary Data Structures Used in Sensor Validation Software

- Dynamic Relation Biasing — In order to get the sensitivity required to detect sensor failures before hard limits (redlines) were exceeded, the significance of engine-to-engine variations in operating conditions had to be understood and addressed. To handle this, the system took several data samples as it entered each steady-state condition and biased the relations accordingly. This biasing was limited, however, to prevent accommodating data from sensors which may have failed during transients (i.e., the bias term was itself thresholded).

- Table Compilation — Since a large portion of the development effort for this system was spent on developing and tuning the relations used in the network, a module was developed to facilitate the specification of the various data structures used in the system. This module takes a text file description of the relations to be used, and compiles all of the tables and constants required by the validation system.

The AREC-hosted SDV system software consisted of about 1,000 lines of C code. It was developed on a Sun SPARCstation using recorded sensor data from SSME tests. The network shown in Figure 10 was used to validate the High Pressure Fuel Turbine Discharge Temperature (HPFT DS T) sensors using six parameters (described in Table 2) and eleven binary empirical relations. This was a fully-connected network with the exception of relations 93/209, 93/210, 130/209, and 130/210 which proved to be very poor predictors and negatively impacted the sensitivity of the system.

The models used in the AREC-hosted SDV system were empirically derived, binary models as indicated by Figure 10. In general, either linear or cubic models were derived. Most relationships involving only pressures and/or speeds appeared linear when cross-plotted. However, relationships involving temperatures (particularly the High Pressure Fuel Turbine Discharge Temperatures) appeared to have a cubic relationship when cross-plotted. The following steps were used in the derivation of these models:

1. Data for several firings were concatenated together into a large training file. For the network shown in Figure 10 the tests used were A1618, A1612, A2492, A2497, and B1072, since these represent one firing from each of the different engines for which data was available. The datasets were first stripped of all data prior to START+7 seconds to remove the startup transient, and all data after the SHUTDOWN command.

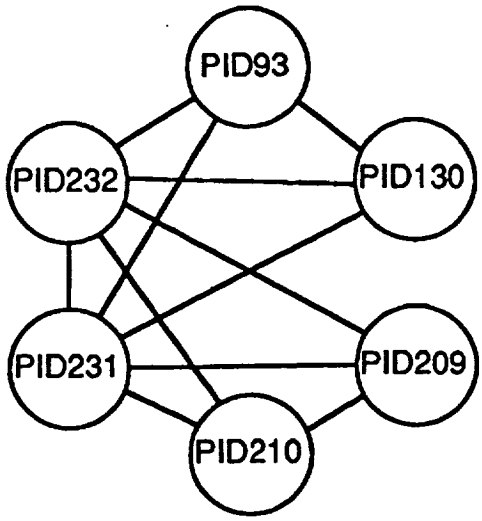

Figure 10. AREC Sensor Validation Network

PID Number	Description
93	PBP Discharge Temp, Ch A
130	MCC Pressure, Ch A1
209	LPOP Discharge Pressure, Ch A
210	LPOP Discharge Pressure, Ch B
231	HPFT Discharge Temp, Ch A
232	HPFT Discharge Temp, Ch B
	Control Signals
280	Vehicle Command (Engine Start/Stop)
287	MCC Pc Control Reference

Table 2. Eight Sensor Channels Used in the AREC-Hosted Sensor Data Validation System

2. A standard linear regression routine was then used to generate both first and third-order polynomial models on the test data for every pair of sensors.
3. The third-order models were converted into four first-order models by evaluating the first derivative at each power level using average values for the sensors involved (referred to as tangent-cubic models). Figure 11 is a graphical depiction of this procedure. This was performed both for run-time efficiency (linear models are less costly to evaluate than cubic ones) and because it was felt that the tangent-cubic models would perform better under anomalous engine conditions than linear models trained on power-level-specific data.
4. A program was run for all relations which computed the average of the residuals for all models at each power level.
5. A subset of the relations derived in steps 2 and 3 was selected for use (in particular, only a first-order OR a tangent-cubic model was used for any given pair of sensors).
6. Initial thresholds were defined for the selected models based on the results of step 4 (initially set at three standard deviations).
7. The assembled SDV system was tested against the full-sample data from the training datasets to ensure that no false alarms were issued.

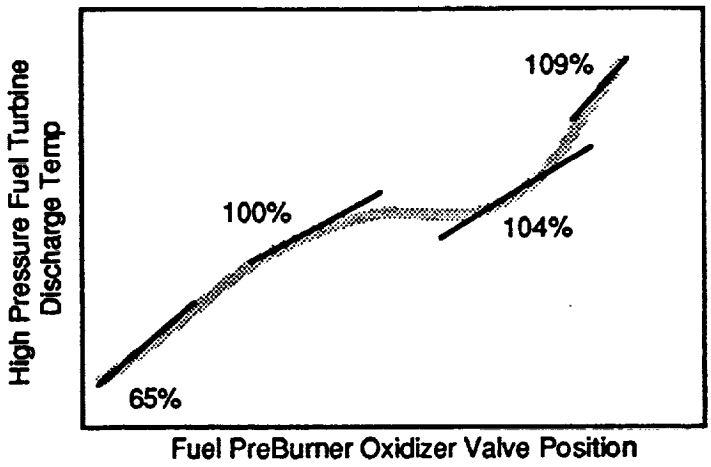

Figure 11. Tangent-Cubic Empirical Model

8. A variant of the SDV system was run to determine the sensitivity of the system in detecting failures in each of the sensors. This was done by setting all sensors to their mean values and then varying one sensor's value incrementally until it was failed (the overall process was repeated for all power levels, for all sensors, and for high and low variations). The mean values were taken from the Phase II SSME Data Base maintained at NASA MSFC (dated 10/13/89). The primary purpose of this test was to ensure that slow drifts in redline sensors would be detected by the sensor validation system before the values reached redline.
9. The model residual thresholds were tuned to ensure maximum sensitivity while ensuring that no false alarms were issued. This involved many iterations through steps 7, 8, and 9. The final thresholds incorporated into the run-time sensor validation system are constant, and do not change between power levels.
10. A program was run to compute the relation biases (model offsets) used on a number of different test datasets. This information was used to set the bias limits. Since there were not enough datasets to obtain a statistically significant sample of biases for each sensor, the limits were empirically set to 150% of the largest bias seen.

The sensor validation system was then tested on three additional validation datasets—A2495, B1069, and B1071—without any false alarms being issued (these were the only additional datasets available at the time; for increased reliability the SDV system should be validated on a much wider range of datasets). In addition, sensitivity analyses were successfully run on all red-line sensors to ensure that the validation system would detect slow drift failures prior to redline exceedance. These tests were performed on the development workstation in a non-real-time environment.

Simulation Laboratory Tests

The sensor validation software was then integrated into the Advanced Rocket Engine Controller and set up in Aerojet's Real-Time Simulation Laboratory. This facility is based on an AD-100 multiprocessor computer, which is capable of either simulating engine firings or replaying data from engine firings in real-time. The AD-100 was programmed to replay recorded data from 10 SSME firings in order to test the AREC and the real-time characteristics of the sensor validation system. The system correctly monitored nine normal

SSME tests in real time without any false alarms being generated. The system correctly detected a hard failure in HPFT DS T on a tenth SSME test dataset.[21] Table 3 summarizes these results.

Test	Duration	Results
A1619	529	No false alarms.
A2497	550	No false alarms.
A2493	550	No false alarms.
B1046	530	No false alarms.
B1064	520	No false alarms.
B1067	700	No false alarms.
B1073	80	No false alarms.
B1075	300	No false alarms.
B1077	513	No false alarms.
A1637		Failure occurred during power level transient. SDV system detected failure 1.48 seconds later, following its post-transient delay and training interval (performed correctly).

Table 3. Simulation Laboratory False Alarm and Hard Failure Detection Test Results

In order to evaluate the sensitivity of the system to "soft" sensor failures in a real-time environment, a series of tests were run in which a slow drift in HPFT DS T (high or low) was simulated by the AD-100 computer while all other sensors were held at their nominal values (engine test data was not used for these tests). The point at which the system disqualified the sensor was then recorded. These tests, summarized in Table 4, indicated that the system had adequate sensitivity to soft failures.

Real-Time Validation on TTB

Following tests in APD's Real-Time Simulation Laboratory, the AREC-based sensor validation system was installed in the Technology Test Bed blockhouse at MFSC to receive and analyze real-time data from TTB hot-fire tests. The same validation network and sensor validation software configuration used in the Simulation Laboratory tests were used at TTB.

Table 5 summarizes the results of the TTB tests. The sensor validation system correctly tracked engine start, stop, and power level transitions, performed bias training, and monitored nominal data without issuing any false alarms. However, none of the monitored sensors experienced failures during the test series, so the sensitivity of the system in the TTB environment could not be established.

II.3. Empirical and Characteristic Modeling

In FY92 Aerojet undertook the task (under the Life Prediction contract) of determining the viability of using analytical redundancy to validate the majority of the sensors used on SSME for control and health monitoring. The basic approach was to identify and investigate sets of engine parameters whose measurements are statistically correlated for a nominal engine firing, or whose measurements are known to be related via first-principle (characteristic) equations.

PID	Drift Direction	Power Level %	Value at Which Sensor Was Disqualified	Criteria for Pass (Redline)
231	High	65	1550	<1850
	"	100	1718	"
	"	104	1761	"
	"	109	1842	"
	Low	65	1406	None
	"	100	1229	"
	"	104	1361	"
	"	109	1384	"
232	High	65	1611	<1960
	"	100	1716	"
	"	104	1798	"
	"	109	1900	"
	Low	65	1400	None
	"	100	1616	"
	"	104	1641	"
	"	109	1710	"

Table 4. Simulation Laboratory Tests of "Soft" Failures via Induced Drifts

Test	Date	Duration (seconds)	Notes
TTB-031	4/15/92	85	Nominal firing. No false alarms, no missed detections.
TTB-032	4/28/92	205	Nominal firing. No false alarms, no missed detections.
TTB-033	5/14/92	18	Ambient powerhead temperature redline cutoff. No false alarms, no missed detections.
TTB-034	5/28/92	210	Nominal firing. No false alarms, no missed detections.
TTB-035	6/11/92	200	Nominal firing. No false alarms, no missed detections.

Table 5. TTB Test Results

Sensor Selection

Table 6 lists the engine parameters and the appropriate sensors investigated in this task. Some of these parameters were selected as being critical to safely operating the engine, including control and redline parameters and those identified for use in advanced safety algorithms. Less critical sensors that might provide additional analytical redundancy coverage were also included. Sensor data is captured by two different systems during an SSME firing: the engine controller relays data from sensors with PID numbers of 300 or less via a Command and Data Simulation (CADS) computer; while sensors with PID numbers over 300 are caputured by the facility data recording system.

Parameter	PID	PIDs Used
High Pressure Fuel Pump (HPFP) Shaft Speed	260,261,764	260,764
High Pressure Fuel Turbine (HPFT) Discharge Temperature	231,232	231,232
HPFP Discharge Pressure	52,459	52
Main Combustion Chamber (MCC) Pressure	129,130,161,162,63	129
Fuel Preburner (FPB) Chamber Pressure	58,410	58
HPFP Coolant Liner Pressure	53,54	53
Oxidizer Preburner (OPB) Chamber Pressure	480	480
FPB Oxidizer Valve Position	42,143,175	42,175
HPFP Inlet Pressure	203,204	203
Oxidizer Flow (Facility)	1212,1213	1212
Fuel Flow (Facility and Engine)	133,253,301, 251,722,1205, 1206	133,722, 1205
MCC Coolant Discharge Pressure	17	17
Low Pressure Fuel Turbine Inlet Pressure	436	436
Low Pressure Fuel Pump (LPFP) Speed	32,754	32
Low Pressure Oxidizer Pump (LPOP) Speed	30,734	30
High Pressure Oxidizer Turbine (HPOT) Discharge Temperature	233,234	233,234
MCC Hot Gas Injection Pressure	24,371	24,371
MCC Oxidizer Injection Temperature	21,595	21
OPB Oxidizer Valve Actuator Position	40,141,176	40,176
MCC Coolant Discharge Temperature	18	18
LPOP Discharge Pressure	209,210	209
Preburner Boost Pump (PBP) Discharge Temperature	93,94	93
MCC Liner Cavity Pressure	1951,1956,1957	1951
HPOP Discharge Pressure	90,334	90,334
PBP Discharge Pressure	59,341	59
HPFP Discharge Temp	659	659
HPOP Inter. Seal Purge Pressure	211,212	211
HPOT Secondary Seal Cavity Pressure	91,92	91
HPFP Inlet Temp	225,226	225
HPOP Balance Cavity Pressure	327,328	327,328
HPFP Balance Cavity Pressure	457	457
HPFP Coolant Liner Temp	650	650
Engine Fuel Inlet Pressure	819,821,827	819
Engine Oxidizer Inlet Pressure	858,859,860	858
HPOP Primary Seal Drain Pressure	951,952,953	951
HPOT Primary Seal Drain Pressure	990	990
Engine Fuel Inlet Temp.	1021,1017,1018	1021,1017
Engine Oxidizer Inlet Temp	1058,1054,1056	1058,1054
HPOT Secondary Seal Drain Temp	1188	1188
HPOT Primary Seal Drain Temp	1190	1190
Fuel Repressure Interface Pressure	835	835

Table 6. Sensors Used in FY92 Modeling Task

The primary objective of this task was to consider the relationships between various engine parameters, thus redundant sensors were typically not evaluated (i.e., only one PID per parameter was used in the analyses). Several redundant measurements were included after an initial analytical and statistical survey identified those which showed significant differences.

Data Preparation

The data sets used consisted of nine nominal test firings for training and two additional test firings for verification. As shown in Table 7, these test cases included various engines including multiple tests with the same engine, thus providing useful information on test to test variations.

Test Firing	Engine	Duration	Use
A2530	2206	300.00 sec	Training
A2536	2206	300.00 sec	Training
A2539	0216	530.00 sec	Training
A2547	2011	420.00 sec	Training
A2548	2206	300.00 sec	Training
B1060	0213	530.00 sec	Training
B1069	0213	700.00 sec	Training
B1077	0213	513.00 sec	Training
B1089	0213	530.00 sec	Training
B1063	0213	513.00 sec	Verification
A2537	2035	300.00 sec	Verification

Table 7. Test Firing Datasets Used in FY92 Modeling Task

The sensor measurements were initially prepared by removing the start transients (first seven seconds after ignition) and the shutdown transients. The data was then smoothed and reduced from approximately one-half million data points per dataset to 50,000 data points per dataset to make the modeling procedures tractable. Only routines which computed model coefficients were run on this reduced data; all other routines, including all validation tests, used the original full sample data.

Empirical Model Ranking

Initially, first and third degree binary curve fits were computed between all pairs of selected PIDs. The curve fits were ranked for each test according to minimal residual variance and the rankings were averaged across the nine training test firings (e.g., if a model had the third lowest residual variation in half of the tests and the fourth lowest residual variation in the other half, its final ranking would be 3.5). As an example, Table 8 lists the top 20 ranked linear and cubic fit parameters for the High Pressure Fuel Pump Speed, Channel A sensor (PID 260). The "rank" column in this table is the averaged rank value described above.

260 RPM HPFP SPEED A

Linear fit ranking.

rank	n	name		
0.00000	9	260	RPM	HPFP SPEED A
1.00000	9	764	RM	HPFP SPD NFD 48KRPM
4.44444	9	659	T2	HPFP DS T CH A 30/560
4.88889	9	129	PSIA	MCC PC A2
5.88889	9	17	PSIA	MCC CLNT DS PR
7.22222	9	436	GP	LPFT IN PR 1 10K PSIS
7.33333	9	133	GPM	FUEL FLOW A1
7.44444	9	722	GM	ENG FL FLOW NFD 29KGPM
7.44444	9	30	RPM	LPOP SPEED
8.00000	9	53	PSIA	HPFP CLNT LNR A
10.0000	9	52	PSIA	HPFP DS PR A
10.8889	9	371	GP	MCC H. G. INJ PR0/5000PS
13.8889	9	1205	GM	FAC FL FLOW 1 22KGPM
14.0000	9	90	PSIA	HPOP DS PR A
15.7778	9	457	GP	HPFP BAL CAV PR 10K PSIS
16.6667	9	328	GP	HPOP BALCAV 2A P5K PSI
16.7778	9	334	AP	HPOP DS PR NFD 7K PSIA
16.7778	9	1212	GM	FAC OX FLOW 1 8500GPM
18.3333	9	835	GP	FL PRESS INT PR 5K PSIG
19.6667	9	58	PSIA	FPB PC A
19.8889	9	327	GP	HPOP BALCAV 1A P5K PSI

Cubic fit ranking.

rank	n	name		
0.00000	9	260	RPM	HPFP SPEED A
1.11111	9	764	RM	HPFP SPD NFD 48KRPM
3.44444	9	129	PSIA	MCC PC A2
4.33333	9	722	GM	ENG FL FLOW NFD 29KGPM
5.77778	9	659	T2	HPFP DS T CH A 30/560
6.00000	9	133	GPM	FUEL FLOW A1
6.66667	9	53	PSIA	HPFP CLNT LNR A
8.33333	9	17	PSIA	MCC CLNT DS PR
9.66667	9	436	GP	LPFT IN PR 1 10K PSIS
9.77778	9	371	GP	MCC H. G. INJ PR0/5000PS
10.1111	9	52	PSIA	HPFP DS PR A
13.0000	9	457	GP	HPFP BAL CAV PR 10K PSIS
13.7778	9	30	RPM	LPOP SPEED
15.1111	9	90	PSIA	HPOP DS PR A
15.6667	9	1205	GM	FAC FL FLOW 1 22KGPM
16.8889	9	32	RPM	LPFP SPEED
17.7778	9	328	GP	HPOP BALCAV 2A P5K PSI
17.8889	9	1212	GM	FAC OX FLOW 1 8500GPM
17.8889	9	334	AP	HPOP DS PR NFD 7K PSIA
19.6667	9	58	PSIA	FPB PC A
20.1111	9	835	GP	FL PRESS INT PR 5K PSIG

Table 8. Ranked Linear and Cubic Fit Parameters for PID 260

These rankings were analyzed and the top three candidate models were selected for each parameter (e.g., the circled PIDs in Table 8). Other than removing redundancies from consideration, parameters were selected on the basis of their ranking and knowledge of nominal SSME operation. For example, in Table 8, PID 129 was not selected because most parameters have a very high correlation with Main Chamber Pressure (almost all measurements in the engine scale up and down with power level) and PID 436 was not selected because the cubic model did not rank well, and because it is "causally remote" from the PID 260 measurement. Attachment 1 presents the selected parameters and a brief rationale for each, the average "rank" value described above, the order of the model selected for use ("1" for linear and "3" for cubic) and an evaluation of the model fit with and without bias training.

Empirical Model Evaluation

The linear and cubic fit coefficients and residual characteristics for the three selected empirical relations for each sensor were then computed. Nine sets of coefficients were computed for each relation by performing linear regression on each of the nine training datasets individually. A composite, or "accumulated" model was then formed for each relation by averaging the coefficients obtained for each training dataset. This accumulated model was then evaluated against each of the training datasets, and the mean and standard deviation of the residual computed. Finally, the average of these means and standard deviations for the accumulated model was computed as a measure of the overall quality of the model.

Tables 9 and 10 show these values for the three selected models for HPFP SPEED CH A (PID 260) in linear and cubic form, respectively. In each of these tables, the "Mean" and "Sigma" values are the mean and standard deviation of the model residual, and "C0", "C1", etc., are the model coefficients (with "C0" being the zero-order coefficient). Note that the dynamic range of PID 260 is 1,350 to 45,000 RPM, so that the seemingly large residual standard deviations are actually only about 1/2% of the sensor's range.

Figures 12-16 are examples of scatter plots* (for the model relating PID 260 to PID 659) which were generated to show how well the empirical relationships fit the data. Figures 12 and 13 are plots for test A2530 which shows how the linear and cubic models fit a single training dataset (with the models constructed on the same dataset). Figures 14 and 15 are scatter plots for averaged relations (i.e., with coefficients averaged over all training tests), evaluated against all test firing data to show the effects of test to test variations. Figure 16 is a scatter plot for the averaged relations evaluated against a single validation test firing dataset (B1063).

Attachment 1 includes some observations from this data. Parameters were identified as good fits if their residual standard deviation was less than 1% of the maximum parameter value (maximum dynamic range of the sensor). Medium fit was associated with a residual standard deviation of 1% - 2.5% of the maximum parameter value, and a poor fit was considered when the residual deviations were in excess of 2.5%. Those parameters that were basically not correlated were identified as unusable.

Attachment 2 presents the averaged coefficients for all selected linear and cubic models.

---

* A single sample of data following the engine shutdown signal was erroneously included in each of the empirical training datasets; these show up on the plots as single outlier data points. It was believed that one data point out of 1200 would not affect the results.

Linear Curve Fit
y-pid = 260 RPM HPFP SPEED A

x-pid = 659 T2 HPFP DS T CHA

Test	Residual Mean	Sigma	C0	C1
a2530	-3.68E-04	2.18E+02	-6.0585E+03	4.3131E+02
a2536	9.25E-04	1.51E+02	-7.0018E+03	4.3608E+02
a2539	-1.68E-04	1.91E+02	-6.6352E+03	4.4143E+02
a2547	3.17E-04	2.78E+02	-7.0957E+03	4.4303E+02
a2548	1.23E-03	1.88E+02	-6.9675E+03	4.3826E+02
b1060	4.24E-04	3.02E+02	-5.7085E+03	4.2960E+02
b1069	3.26E-03	2.75E+02	-5.6677E+03	4.2677E+02
b1077	-4.25E-04	3.21E+02	-5.4051E+03	4.2730E+02
b1089	-2.04E-03	1.75E+02	-5.3045E+03	4.0703E+02
Accum	-1.98E+01	6.19E+02	-6.2050E+03	4.3120E+02

x-pid = 17 PSIA MCC CLNT DS PR

Test	Residual Mean	Sigma	C0	C1
a2530	1.93E-03	2.61E+02	1.3163E+04	4.9021E+00
a2536	1.63E-03	1.97E+02	1.3155E+04	5.0277E+00
a2539	1.84E-03	2.62E+02	1.3296E+04	4.9604E+00
a2547	1.06E-03	3.33E+02	1.3113E+04	4.8169E+00
a2548	-5.66E-04	3.07E+02	1.3155E+04	4.9314E+00
b1060	1.23E-03	3.06E+02	1.2835E+04	4.9736E+00
b1069	1.10E-03	2.59E+02	1.2867E+04	4.9860E+00
b1077	-9.70E-04	3.18E+02	1.3640E+04	4.6331E+00
b1089	-2.03E-03	2.62E+02	1.2837E+04	4.8696E+00
Accum	-2.07E+01	4.82E+02	1.3118E+04	4.9001E+00

x-pid = 133 GPM FUEL FLOW A1

Test	Residual Mean	Sigma	C0	C1
a2530	-1.17E-03	2.65E+02	1.2923E+04	1.3551E+00
a2536	8.78E-04	2.22E+02	1.3077E+04	1.3663E+00
a2539	1.10E-03	2.40E+02	1.2936E+04	1.3763E+00
a2547	1.37E-03	3.36E+02	1.2968E+04	1.3653E+00
a2548	-5.27E-04	2.93E+02	1.2785E+04	1.3714E+00
b1060	3.04E-03	3.10E+02	1.3289E+04	1.3542E+00
b1069	5.16E-04	2.59E+02	1.3154E+04	1.3614E+00
b1077	4.01E-04	3.20E+02	1.3383E+04	1.3426E+00
b1089	-2.09E-04	2.81E+02	1.3223E+04	1.3651E+00
Accum	-4.93E+00	3.13E+02	1.3082E+04	1.3620E+00

Table 9. Linear Empirical Fit Coefficients for PID 260

Third Order Curve Fit

y-pid = 260 RPM HPFP SPEED A

x-pid = 659 T2 HPFP DS T CHA

Residual

Test	Mean	Sigma
a2530	-1.47E-02	1.53E+02
a2536	-1.64E-03	6.19E+01
a2539	5.66E-03	1.48E+02
a2547	1.56E-02	1.43E+02
a2548	-3.38E-03	7.00E+01
b1060	1.23E-02	2.93E+02
b1069	-3.16E-03	2.46E+02
b1077	-4.89E-03	3.08E+02
b1089	-6.63E-03	1.19E+02
Accum	1.35E+01	5.31E+02

Test	C0	C1	C2	C3
a2530	5.2353E+04	-1.8947E+03	3.0175E+01	-1.2796E-01
a2536	5.1549E+04	-1.8052E+03	2.8182E+01	-1.1648E-01
a2539	3.8672E+04	-1.3295E+03	2.2643E+01	-9.4948E-02
a2547	6.2633E+04	-2.3689E+03	3.6800E+01	-1.5701E-01
a2548	4.8362E+04	-1.6841E+03	2.6777E+01	-1.1117E-01
b1060	6.4350E+04	-2.3934E+03	3.6885E+01	-1.5718E-01
b1069	7.7948E+04	-2.9436E+03	4.4085E+01	-1.8807E-01
b1077	5.6826E+04	-2.0473E+03	3.1907E+01	-1.3412E-01
b1089	5.0955E+04	-1.7056E+03	2.5870E+01	-1.0371E-01
Accum	5.5961E+04	-2.0192E+03	3.1481E+01	-1.3229E-01

x-pid = 17 PSIA MCC CLNT DS PR

Residual

Test	Mean	Sigma
a2530	-5.24E-03	2.29E+02
a2536	-1.30E-03	1.67E+02
a2539	5.31E-03	1.68E+02
a2547	3.81E-03	1.40E+02
a2548	-2.28E-03	2.50E+02
b1060	-1.07E-02	2.93E+02
b1069	5.54E-03	2.38E+02
b1077	5.09E-03	3.06E+02
b1089	-7.51E-03	1.24E+02
Accum	-2.52E+01	5.13E+02

Test	C0	C1	C2	C3
a2530	-8.1156E+03	2.1424E+01	-4.1676E-03	3.4339E-07
a2536	-2.2078E+03	1.7063E+01	-3.0331E-03	2.4769E-07
a2539	-2.5454E+04	3.5670E+01	-7.9006E-03	6.6387E-07
a2547	-4.4082E+04	4.9817E+01	-1.1386E-02	9.3559E-07
a2548	-1.7856E+04	3.0336E+01	-6.7359E-03	5.8198E-07
b1060	-4.5246E+04	5.1827E+01	-1.2376E-02	1.0740E-06
b1069	-3.9595E+04	4.7428E+01	-1.1247E-02	9.7927E-07
b1077	-1.2878E+04	2.3676E+01	-4.4670E-03	3.4380E-07
b1089	-6.2965E+04	6.4931E+01	-1.5588E-02	1.3289E-06
Accum	-2.8711E+04	3.8019E+01	-8.5447E-03	7.2206E-07

Table 10. Cubic Empirical Fit Coefficients for PID 260

Third Order Curve Fit
y-pid = 45 260 RPM HPFP SPEED A

x-pid = 23 133 GPM FUEL FLOW A1

Test	Residual Mean	Sigma
a2530	3.29E-03	2.04E+02
a2536	1.05E-02	1.77E+02
a2539	-4.63E-03	1.20E+02
a2547	9.46E-03	1.42E+02
a2548	5.91E-03	2.01E+02
b1060	-1.51E-02	2.91E+02
b1069	-1.11E-02	2.29E+02
b1077	-7.02E-03	3.08E+02
b1089	1.88E-03	1.32E+02
Accum	-1.79E+01	2.82E+02

Test	C0	C1	C2	C3
a2530	-2.8979E+04	1.0810E+01	-6.9746E-04	1.6863E-08
a2536	-1.8418E+04	8.4511E+00	-5.1906E-04	1.2443E-08
a2539	-3.4949E+04	1.2037E+01	-7.7387E-04	1.8400E-08
a2547	-5.2971E+04	1.6344E+01	-1.0989E-03	2.6247E-08
a2548	-3.2900E+04	1.1827E+01	-7.7853E-04	1.8946E-08
b1060	-6.2824E+04	1.8687E+01	-1.2922E-03	3.1627E-08
b1069	-5.6651E+04	1.7296E+01	-1.1915E-03	2.9255E-08
b1077	-3.2726E+04	1.1506E+01	-7.3309E-04	1.7345E-08
b1089	-7.3562E+04	2.1184E+01	-1.4824E-03	3.6404E-08
Accum	-4.3776E+04	1.4238E+01	-9.5189E-04	2.3059E-08

Table 10. Cubic Empirical Fit Coefficients for PID 260, cont'd

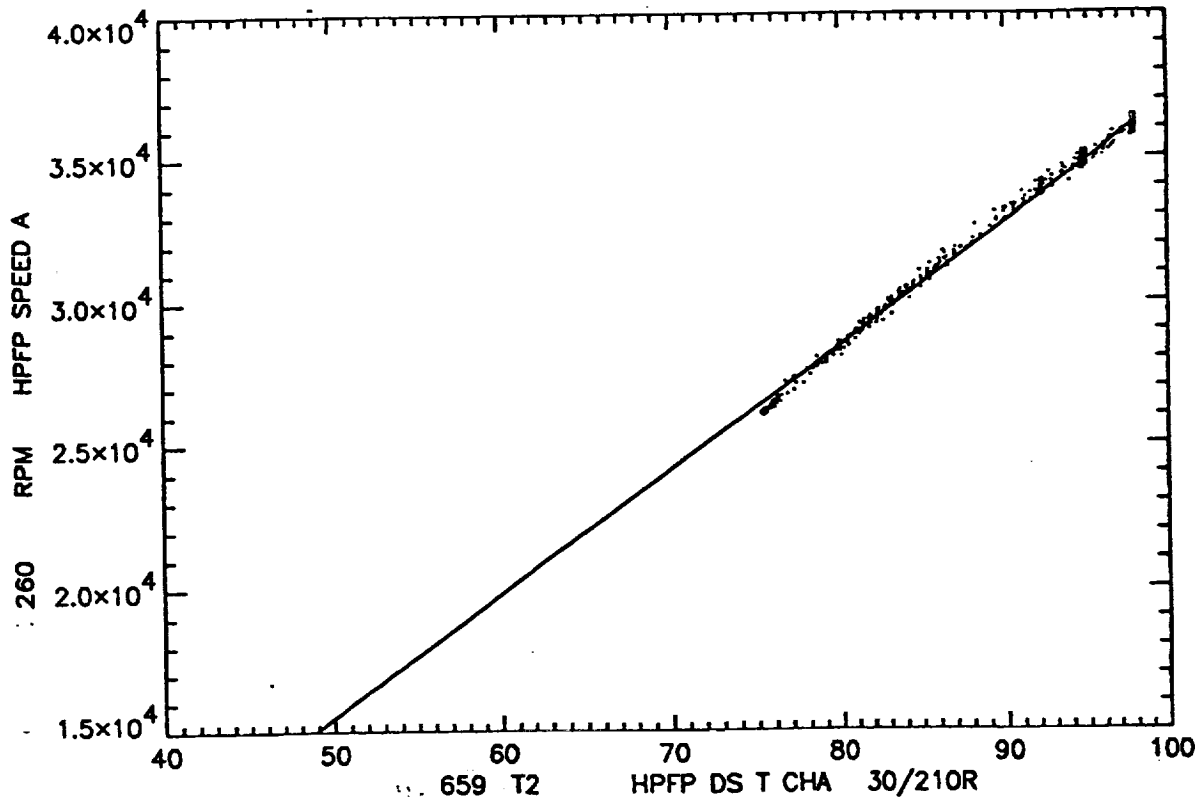

Figure 12. Linear Model Relating PIDs 260 and 659 for Test A2530

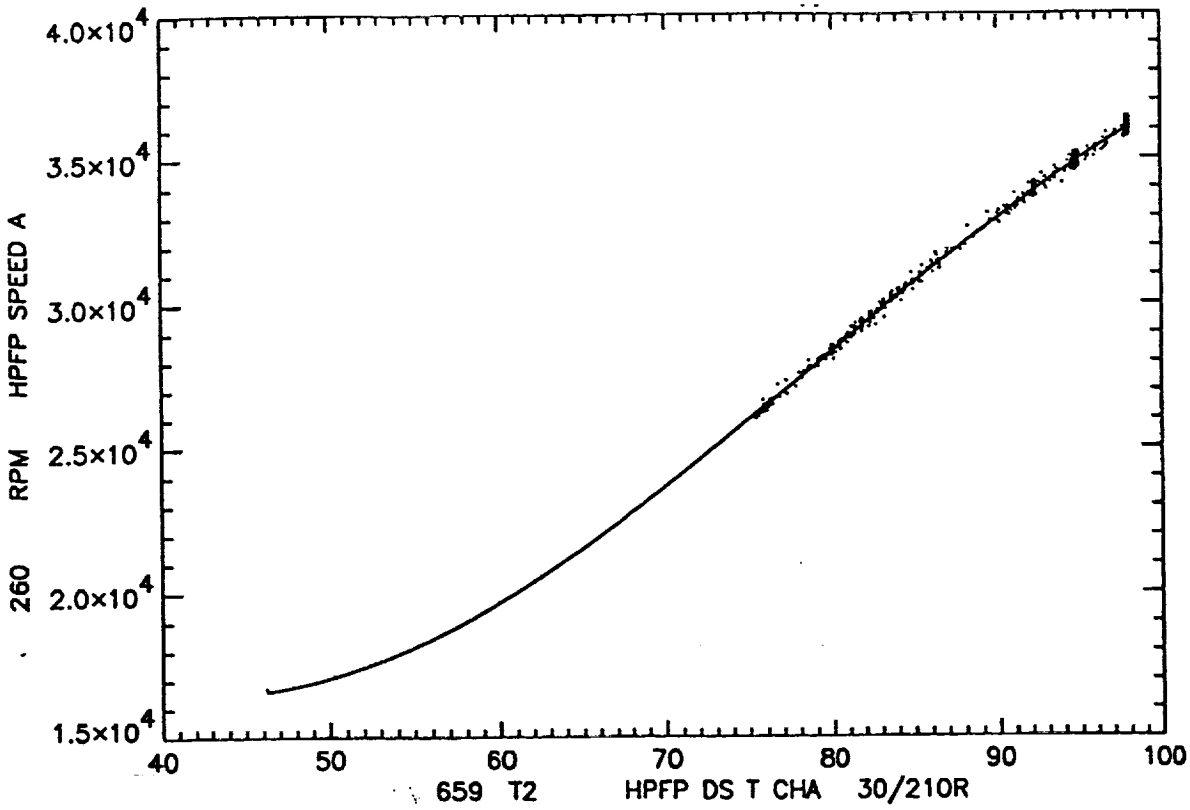

Figure 13. Cubic Model Relating PIDs 260 and 659 for Test A2530

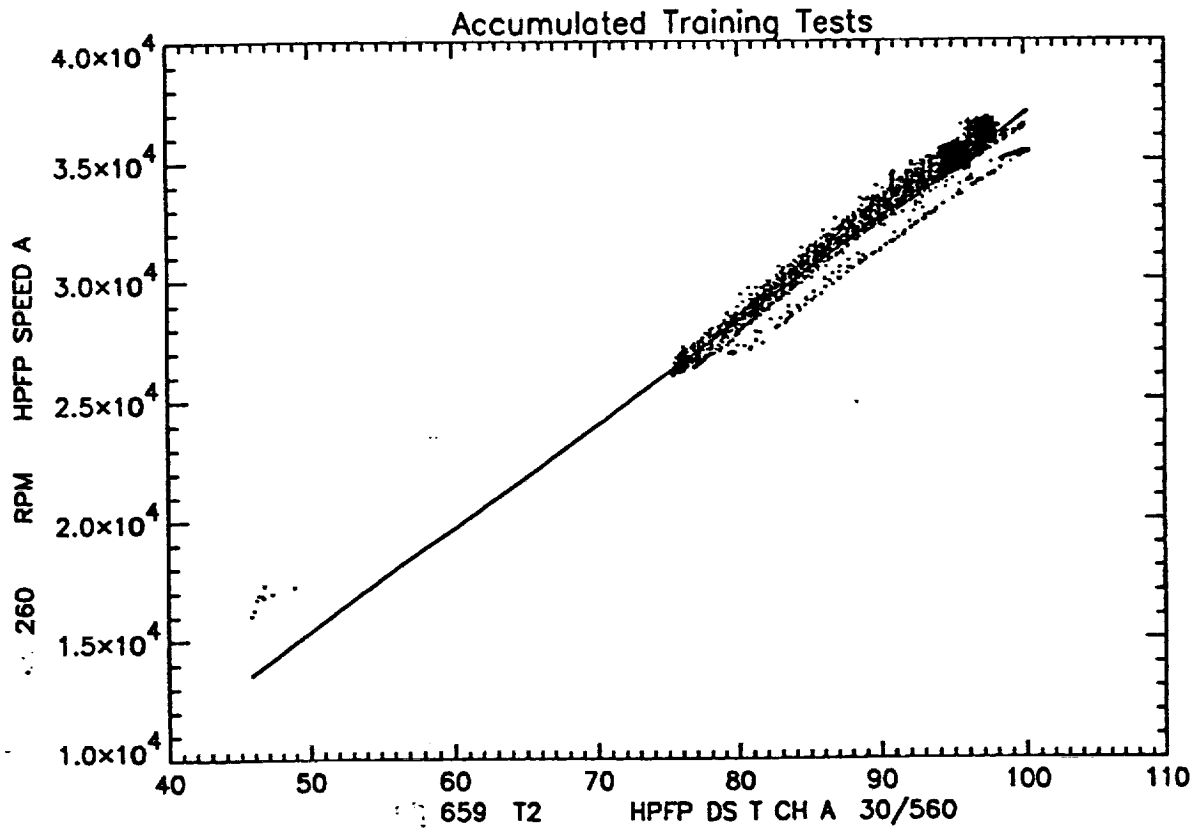

Figure 14. Averaged Linear Model Relating PIDs 260 and 659

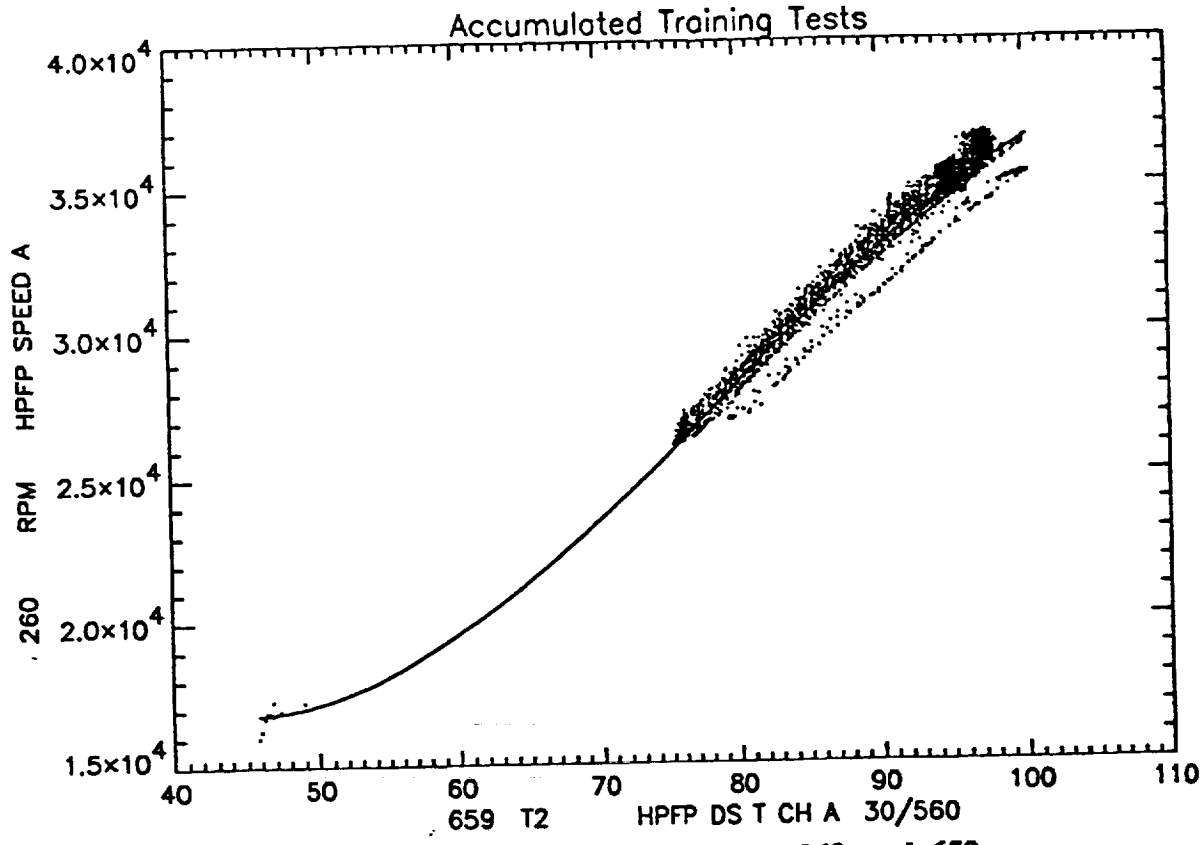

Figure 15. Averaged Cubic Model Relating PIDs 260 and 659

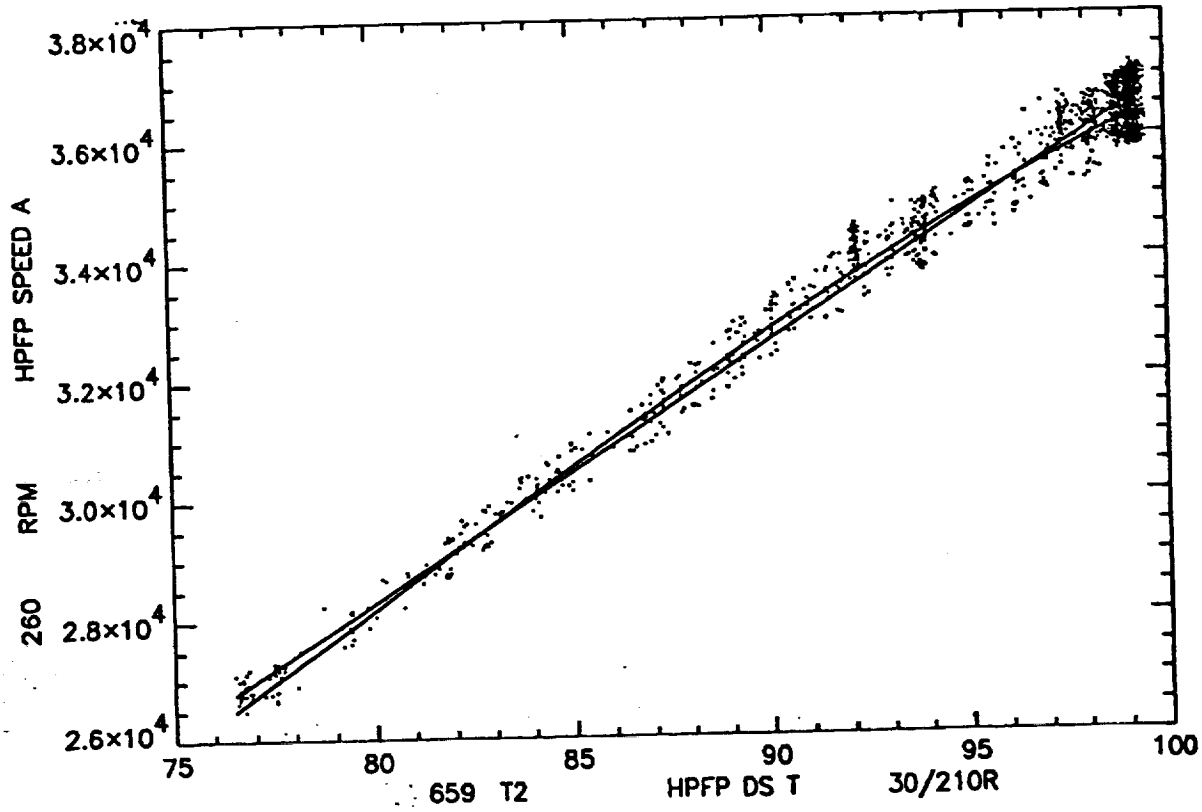

Figure 16. Validation of Models Relating PIDs 260 and 659 on Test B1063

Characteristic Equation Selection.
The characteristic relations were identified through consideration of available sensors and knowledge of engine first principles. Of those considered, the sparsity of sensors on the SSME allowed only three types to be applied: pump flow to impeller speed, pressure rise across a pump to the square of its speed; and line resistance (pressure drop to the flow squared). Table 11 summarizes the characteristic equations considered. The components referred to are: High Pressure Oxidizer Pump (HPOP); High Pressure Fuel Pump (HPFP); Low Pressure Oxidizer Pump (LPOP); Low Pressure Fuel Pump (LPFP); Low Pressure Fuel Turbine (LPFT); and Main Combustion Chamber (MCC). In addition, "DS P" and "IN P" refer to discharge pressure and inlet pressure, respectively. The last three models for line resistances are approximations because not all instrumentation required was available for true first principle relationships.

Model #	Equation	Form
1,2	$\frac{\text{Fuel Flow}}{\text{LPFP Speed}} = \text{constant}$	Pump Affinity
3,4	$\frac{\text{LOX Flow}}{\text{LPOP Speed}} = \text{constant}$	Pump Affinity
5,6	$\frac{\text{Fuel Flow}}{\text{HPFP Speed}} = \text{constant}$	Pump Affinity
7,8,9	$\frac{\text{LPOP DS P - Eng LOX IN P}}{\text{LPOP Speed}^2} = \text{constant}$	Pump Affinity
10,11,12	$\frac{\text{HPFP IN P - Eng Fuel IN P}}{\text{LPFP Speed}^2} = \text{constant}$	Pump Affinity
13,14,15	$\frac{\text{HPFP DS P - HPFP IN P}}{\text{HPFP Speed}^2} = \text{constant}$	Pump Affinity
16,17,18	$\frac{\text{HPOP DS P - MCC Pc}}{\text{LOX Flow}^2} = \text{constant}$	Line Resistance
19,20,21	$\frac{\text{MCC Coolant DS P - LPFT IN P}}{\text{LPFP Speed}^2} = \text{constant}$	Line Resistance
22,23,24	$\frac{\text{HPOP DS P - LPOP DS P}}{\text{LPOP Speed}^2} = \text{constant}$	Line Resistance

Table 11. Characteristic Equations Evaluated

Characteristic Equation Fit
Attachment 3 provides details of the characteristic equations evaluated and the coefficients derived from the training datasets. The models coefficients shown have been averaged over all training datasets in the same manner as the "accumulated" empirical models. As an example, Table 12 shows the derived coefficients for the characteristic equation relating LOX Flow and LPOP Speed. In each of these tables, the "Mean" and "Sigma" values are the mean and standard deviation of the model residual, and "C0", "C1", etc., are the model coefficients. The large residual means and relatively small residual standard deviations for these models indicate that constant offsets (a zero-order term in the equation) should always be used, even though the first principle relations do not specify their use. Offsets for the accumulated (averaged) characteristic models should simply be the average of the residual means computed.

Figures 17-19 are examples of the scatter plots generated during the study to show the quality of characteristic relations when used as predictive models. Figure 17 is a plot for

Characteristic Relation
Fac LOX Flow/ Lpop Spd = constant

PID 1212 : Fac LOX Flow
PID 30 : Lpop Spd

Characteristic Curve Fit
PID 1212 = c1 * PID 30

Test	Residual Mean	Sigma	C1	C1 S.Err
a2530	-3.16E+03	6.47E+01	1.7572E+00	4.29E-03
a2536	-2.97E+03	4.35E+01	1.7047E+00	2.10E-03
a2539	-3.08E+03	3.83E+01	1.7262E+00	3.16E-03
a2547	-3.12E+03	4.52E+01	1.7812E+00	4.95E-03
a2548	-2.89E+03	4.97E+01	1.6816E+00	3.59E-03
b1060	-3.18E+03	4.30E+01	1.7374E+00	3.72E-03
b1069	-3.21E+03	5.06E+01	1.7414E+00	3.74E-03
b1077	-3.30E+03	4.78E+01	1.7637E+00	2.67E-03
b1089	-3.38E+03	3.88E+01	1.8136E+00	4.79E-03
Accum	-3.14E+03	1.04E+02	1.7452E+00	1.41E-03

Characteristic Curve Fit
PID 30 = c1 * PID 1212

Test	Residual Mean	Sigma	C1	C1 S.Err
a2530	1.82E+03	3.67E+01	5.6549E-01	1.38E-03
a2536	1.75E+03	2.55E+01	5.8541E-01	7.21E-04
a2539	1.80E+03	2.21E+01	5.7762E-01	1.06E-03
a2547	1.76E+03	2.53E+01	5.5966E-01	1.56E-03
a2548	1.73E+03	2.95E+01	5.9330E-01	1.27E-03
b1060	1.89E+03	2.45E+01	5.6574E-01	1.21E-03
b1069	1.88E+03	2.89E+01	5.6776E-01	1.22E-03
b1077	1.90E+03	2.70E+01	5.6168E-01	8.51E-04
b1089	1.88E+03	2.14E+01	5.4902E-01	1.45E-03
Accum	1.82E+03	5.99E+01	5.6952E-01	1.68E-04

Table 12. Characteristic Equation Coefficients for LPOP Equation #3

test A2530 which shows how the characteristic equation fits a single training dataset (with the model constructed on the same dataset). Figure 18 is a scatter plot with model coefficients averaged over all training tests and evaluated against all test firing data. Figures 19 and 20 are scatter plots for the averaged model evaluated against individual validation test firings. Table 13 is an evaluation of all characteristic equations considered.

Results of Empirical Modeling

Relations were successfully developed for 33 of the 53 parameters analyzed using linear and cubic binary models. Of the remaining 20 parameters, two were found to be

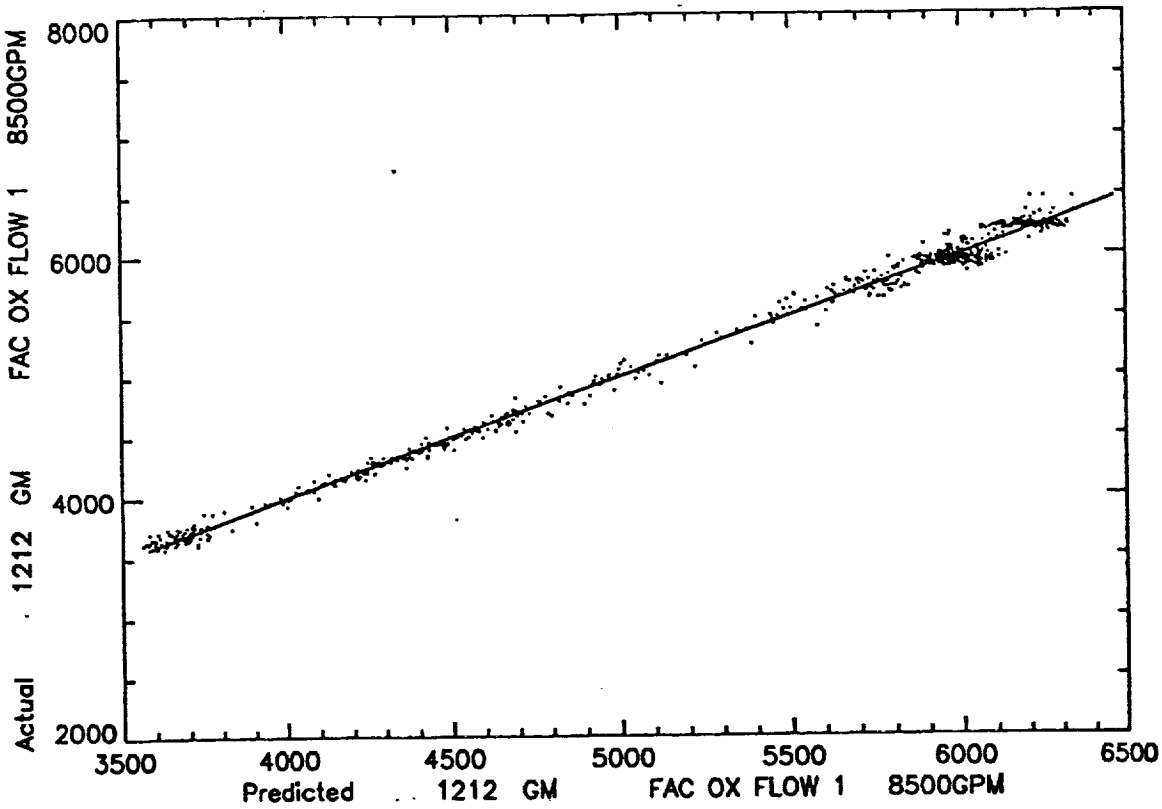

Figure 17. Model for LPOP Equation #3 for Test A2530

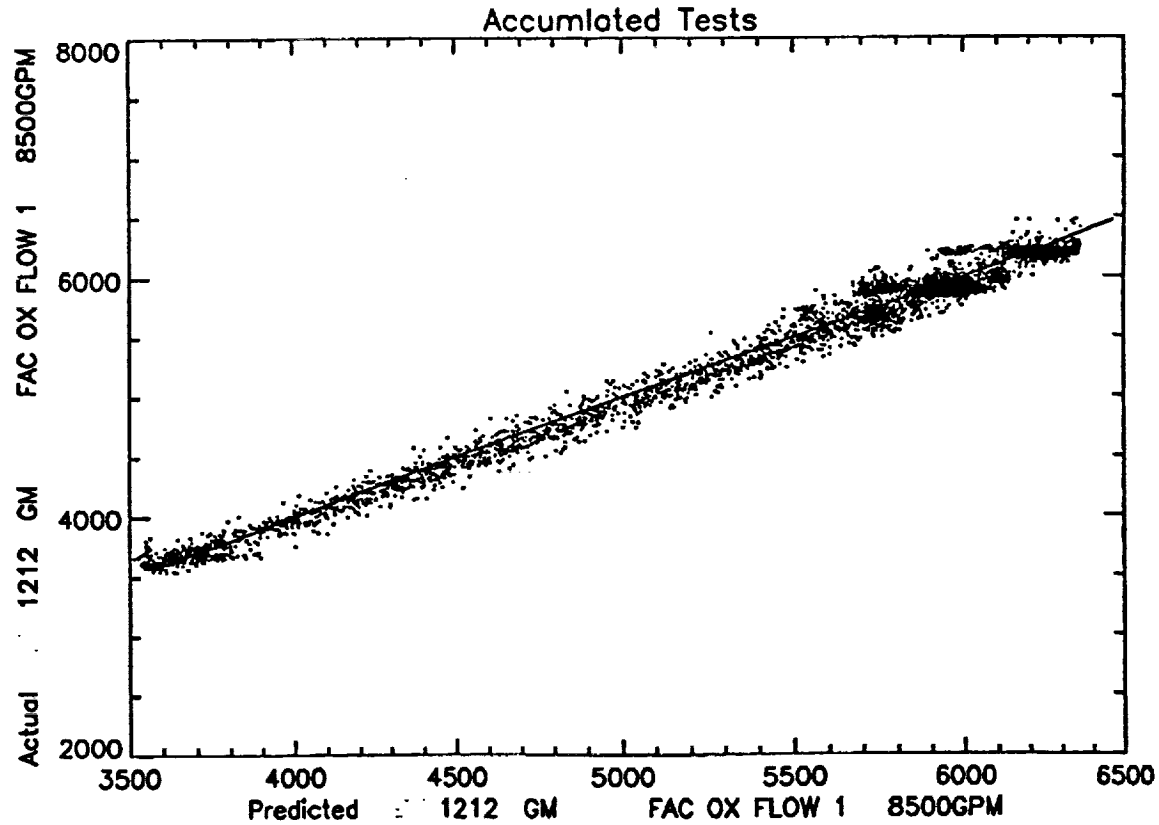

Figure 18. Averaged Model for LPOP Equation #3

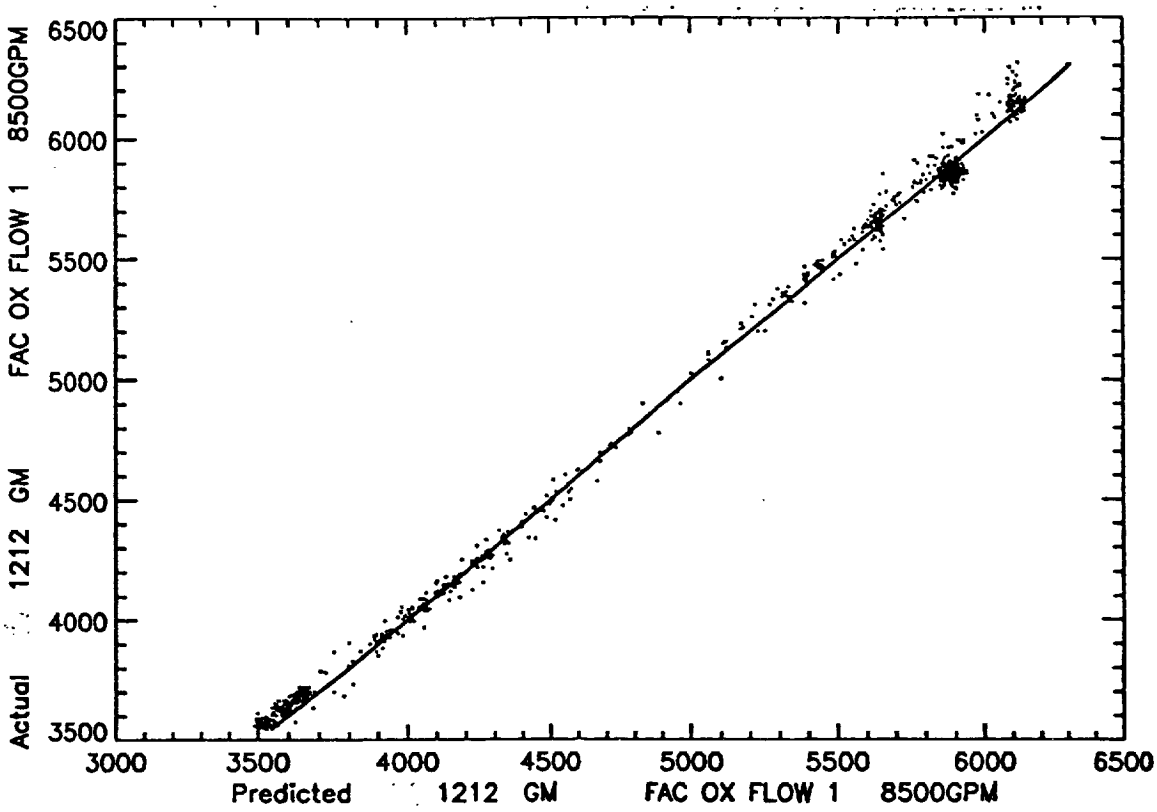

Figure 19. Validation of LPOP Equation #3 on Test A2537

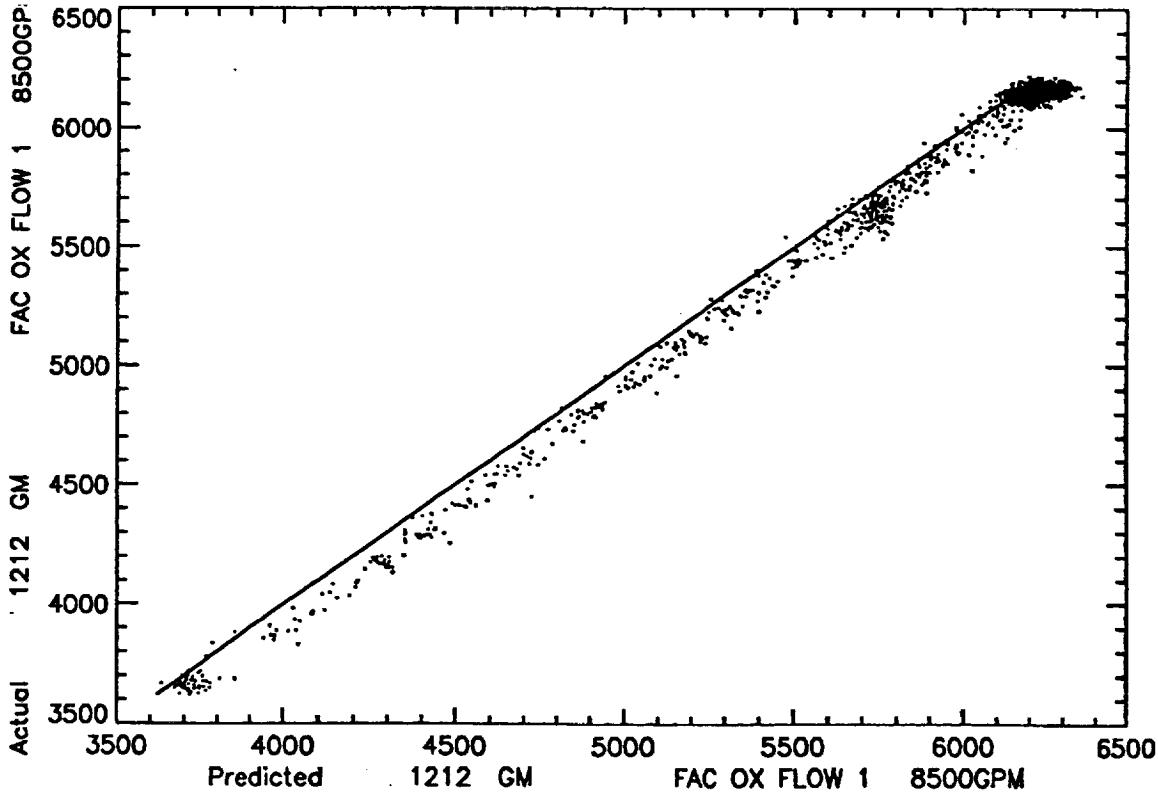

Figure 20. Validation of LPOP Equation #3 on Test B1063

Eqn No	PID	Comments
1.	1205	Poor fit. Bias training will help.
2.	32	Medium fit. Bias training may help.
3.	1212	Medium fit.
4.	30	Medium fit.
5.	1205	Good fit.
6.	260	Medium fit.
7.	209	Good to medium fit.
8.	858	Medium to poor fit. Bias training may help.
9.	30	Poor fit. Bias training may help.
10.	203	Poor fit. Bias training may help.
11.	819	Very poor fit.
12.	32	Poor fit. Bias training may help.
13.	52	Medium to good fit. Bias training may help.
14.	203	Poor fit. Bias training may help.
15.	260	Medium fit. Bias training may help.
16.	90	Good fit.
17.	129	Good fit.
18	1212	Good fit.
19	17	Good fit. Bias training will help. PID32 relation not helpful.
20.	436	Good fit. Bias training will help. PID32 relation not helpful.
21	32	Medium fit.
22	90	Medium fit. Bias training will help.
23	209	Poor fit.
30	30	Medium fit. Bias training will help.

Table 13. Characteristic Equation Observations

anomalous (PID 24 and PID 328*) and six parameters appeared amenable to multi-parameter regression modeling (i.e., PIDs 203, 233, 234, 209, 819, and 858 appear to be a function of more than any one other parameter). The remaining 12 PIDs (18, 1951, 211, 225, 650, 951, 1021, 1017, 1058, 1054, 1188, and 1190) essentially did not correlate well to any other measurements. A good example of this set is PID 1951 (MCC LINER CAV P). According to SSME data analysts, this measures the pressure in a cavity between the inside of the MCC and the outer wall of the combustion chamber. The normal behavior for this sensor is to drop during start (as the MCC heats up, the cavity pulls a vacuum and the pressure drops) and then level off for the rest of the test. This parameter's value is thus primarily a function of time from START. These measurements which do not correlate well to other parameters can be dropped from the list of sensors evaluated by the SDV system, unless they are needed for control, redline, or health monitoring purposes, in which case a more focused modeling effort will need to be undertaken.

* At the completion of the analyses it was discovered that anomalous data from these two PIDs had been included in the training datasets.

In summary, a large percentage of the sensors on SSME can be successfully modeled using linear and cubic polynomial regression techniques. The remaining sensors could be modeled using multi-parameter models, or other forms of models such as time-based models of nominal behavior, or more advanced models such as neural networks. For parameters which are relatively constant during a nominal engine firing and which exist primarily to detect specific failure modes (e.g., PID 1951 exists primarily to detect MCC burn-through), models may be developed by using data from engine anomalies or failure simulations.

Results of Characteristic Modeling

First-principle models are difficult to derive for the SSME due to the scarcity of sensors relative to the complexity of the engine. In taking a very conservative approach, only 7 characteristic equations (with 30 parameter variations) could be fully justified as physically sound. Only one of these 7 equations failed to provide any useful predictive models (models 10, 11, and 12, relating pressure drop across LPFP to the square of LPFP SPEED).

II.4. Summary of Work to Date

The fundamental idea of using analytical redundancy to perform sensor data validation in real time on the SSME has been demonstrated by the work performed on this project. However, while obtaining models for the majority of sensors used for control, redline, and health monitoring purposes appears to be straightforward, a small set of sensors may require extra modeling work if they are to be kept in the validation network.

III. Guidelines for the Development of SDV Models

The TTB tests of the AREC-hosted sensor validation system demonstrated the reliability of using analytical redundancy for SDV. In addition, the SSME data analysis work performed in FY92 demonstrated that models can be derived for most of the sensors of interest, thus establishing that a real-time SDV system can be constructed for the SSME. This section presents a few guidelines which help ensure the proper construction of the analytical redundancy models and validation network used in an SDV system.

III.1. Sensor vs. Plant Anomaly Discrimination

There should be some guarantee that when an engine experiences an anomaly or failure, the validation system will not disqualify all of the sensors measuring the phenomenon when they suddenly start reading grossly abnormal values; this is the essence of the sensor versus plant anomaly discrimination problem.

The analytical redundancy approach taken in this project can correctly handle plant vs. sensor failure discrimination as long as all relations used are guaranteed to hold across all normal operating conditions of the engine, and the validation network is structured so that no single engine anomaly will invalidate enough of the relations involving a particular sensor to disqualify that sensor. If these two conditions are maintained, then the likelihood of the SDV system disqualifying a sensor in response to an engine anomaly is extremely low; on the same order as a simultaneous multiple-point engine failure.

For example, Figure 21 shows the sensor validation network used in previous examples. In this network an anomaly in either pump alone (e.g., cavitation) would not cause the SDV system to disqualify S1. An anomaly in the low pressure pump may invalidate R2, and an anomaly in the high pressure pump may invalidate R4, but both anomalies would need to occur simultaneously (along with a significant discrepancy between S1 and S2) before the SDV system would disqualify S1. Such an occurrence would constitute a "triple-point failure" in the system, which has a very remote possibility of occurrence.

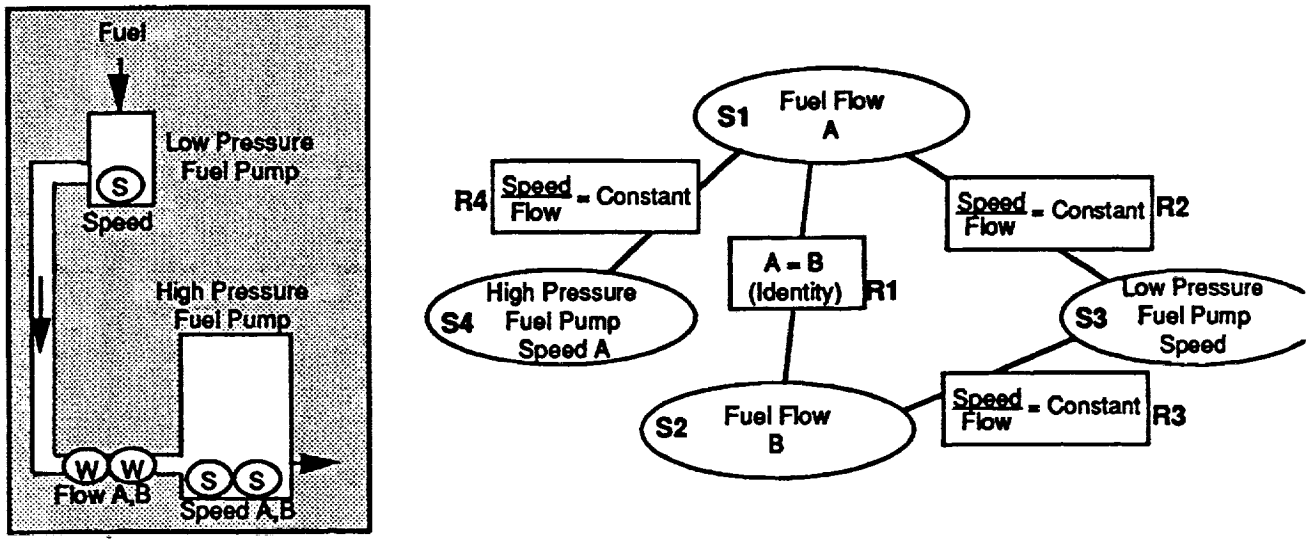

Figure 21. Plant vs. Sensor Failure Example

III.2. Statistical Independence of Sensor Failures

The Bayesian approach to information fusion assumes that sensor failures are independent events. In actuality, there may be events which affect the status of several sensors, requiring changes in the Bayesian Belief Network and subsequent analyses (e.g., loss of an I/O board). Some initial work has been performed by De Bruyne at U.C. Berkeley to study this problem,[9] and the results indicate that the independence assumption is justified (i.e., that introducing events which affect several sensors into the analysis does not significantly affect the results).

However, the statistical independence assumption can be violated by poor construction of the validation network. Figure 22. shows a worst-case example. The network is constructed to validate sensors S1 and S2, using relations R1, R2, and R3; cross-checking against each other and several other sensors (S3-S8). In this example, S1 and S2 rely exclusively on common information for validation. In this network, if there were a failure in either S1 or S2, it would be impossible to determine which of them had actually failed (the current algorithm would fail one arbitrarily, and then continually validate the other, because there would not be any information to disqualify it after R1, R2, and R3 were invalidated).

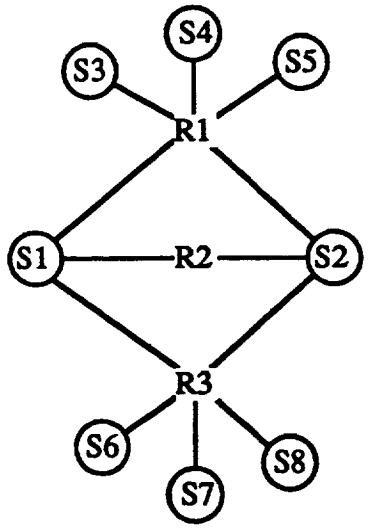

Figure 22. Worst-Case Validation Network

This problem can be avoided through careful construction of the network. However, if only binary relations are used, it is impossible to construct a network in which the independence assumption is violated (assuming that only one relation can be used between any pair of sensors).

III.3. Adapting Models to New Line Replaceable Units

As with most advanced systems, the SSME is not a static design. Components are continually being re-designed and improved, and in some cases completely replaced. In addition, engines of the same design can behave quite differently from one to another. In order for the sensor validation system to retain its fidelity without causing false alarms in the face of such changes in hardware configuration, the software must be set up so that the analytical redundancy models can be quickly tuned when data becomes available from these new configurations.

III.4. Summary

The issues addressed in this section imply the following guidelines in developing analytical redundancy models and in configuring the validation network:

- Models must hold over the widest possible range of normal plant behavior. This implies that characteristic (first principle) models should be used whenever possible, and that all models should be trained on as many datasets as possible. Even though empirical models often seem to fit SSME data with more fidelity than characteristic models, there is a higher degree of confidence that characteristic models will continue to hold during anomalous engine conditions which were not present in the training datasets used to derive empirical models.
- Models with minimum cardinality (i.e., which relate the minimum number of sensors) should be preferred over those with higher cardinality. The lower the cardinality, the greater the guarantee that the statistical independence assumption will hold, and that the system will properly discriminate between plant and sensor failures.
- A tool should be developed which assesses the degree to which the statistical independence assumption is violated for any validation network configuration. The tool must verify that for any single sensor failure the system must be able to: 1) uniquely identify the failed sensor; and 2) continue validating the rest of the sensors in the network.
- The model-building software should be developed so that all models can be quickly reconstructed on new data following a design change or first test of a new engine.

IV. FY93-95 Task Description

This section briefly describes the technical goals of the FY93-95 Real-Time Sensor Data Validation task, and the design extensions to the AREC-based software required to meet them.

IV.1. Scope

The primary goal of the FY93-95 task is to scale up the eight-channel sensor validation system developed and tested on the AREC to validate approximately 97 channels of data from the SSME in real-time (see Table 14.). Fundamentally, this will not require any changes to the run-time algorithms, or to the established methodology for developing and validating analytical redundancy models or for tuning and validating the network.

IV.2. Hard Failure Detection in Redline Sensors

The AREC-hosted SDV system utilized a 3-of-5 multi-cycle strategy (a sensor must be flagged on 3 out of 5 consecutive cycles in order to be disqualified). Unfortunately, the SSME controller will react if a sensor is over redline on two of three consecutive cycles. Thus, to prevent erroneous engine shutdowns the SDV system must be able to detect "hard" sensor failures within two cycles for all redline sensors (at a minimum).

The proposed approach to detecting hard sensor failures is to determine if a sensor's rate-of-change has exceeded a threshold amount over two consecutive cycles (i.e., threshold on the magnitude on cycle 2 less the magnitude on cycle 0). If this condition holds, and the validation network flags the sensor as anomalous during each of the two cycles, then the sensor will be disqualified with a hard failure. For the ground test configuration, the SDV system will still disqualify sensors with hard failures after two consecutive anomalous readings, but since data is only available to ground test computers on alternate controller cycles the SDV system will actually be disqualifying such sensors following four controller cycles in which the sensor is bad.

IV.3. Operation During Power-Level Transients

The AREC-based SDV system did not operate during engine start, shutdown, or power level transitions. The new SDV system will operate, at a minimum, on the latter of these transients. Thus, the system will be in continuous operation from approximately four seconds after mainstage has been achieved until the shutdown signal is detected.

To accomplish monitoring through mainstage power level transitions, the SDV system will utilize multiple sets of model thresholds and hard failure excursion thresholds. One set of thresholds will be used during steady-state (as in the AREC-hosted system), while other thresholds will be used during engine transients and during the bias training period at the start of each steady-state interval. These transient thresholds will undoubtedly be looser constraints on engine behavior. While the SDV system will not be as sensitive to soft sensor failures during the transient intervals, it will still be able to catch hard failures following two samples of anomalous data.

IV.4. Operation During START Transient

As options to this task, the SDV system may be extended to monitor during the engine start-up transient. While the basic approach to SDV is still applicable during start, the models required to successfully cross-check sensors may become extremely complex in order to take dynamic effects into account. Thus, the bulk of these optional tasks will be in the development, test, and integration of new models which will utilize data trends and temporal information, as opposed to the steady-state models which constitute the bulk of the network used for mainstage.

Parameter	PID
MCC Pressure	129,130,161,162,63
OPOV Actuator Position	40,141,176
FPOV Actuator Position	42,143,175
CCV Actuator Position	45,146,174
MOV Actuator Position	38,139,173
MFV Actuator Position	36,137,172
HPFP Inlet Temperature	225,226
HPFP Inlet Pressure	203,204
Engine Fuel Flow	133,253,301,251,722
HPFTP Shaft Speed	260,261,764
HPFT Discharge Temperature	231,232
HPFP Discharge Pressure	52,459
FPB Chamber Pressure	58,410
HPFP Coolant Liner Pressure	53,54
OPB Chamber Pressure	480
Facility Fuel Flow	1205,1206
Facility LOX Flow	1212,1213
MCC Coolant Discharge Pressure	17
LPFT Inlet Pressure	436
LPFP Speed	32,754
LPOP Speed	30,734
HPOT Discharge Temperature	233,234
MCC Hot Gas Injection Pressure	24,367,371
MCC LOX Injection Temperature	21,595
MCC Coolant Discharge Temperature	18
LPOP Discharge Pressure	209,210
PBP Discharge Temperature	93,94
MCC Liner Cavity Pressure	1951,1956,1957
HPOP Discharge Pressure	90,334
PBP Discharge Pressure	59,341
HPFP Discharge Temperature	659
HPOP Intermediate Seal Purge Pressure	211,212
HPOT Secondary Seal Cavity Pressure	91,92
HPOP Balance Cavity Pressure	327,328
HPFP Balance Cavity Pressure	457
HPFP Coolant Liner Temperature	650
Engine Fuel Inlet Pressure	819,821,827
Engine Oxidizer Inlet Pressure	858,859,860
HPOP Primary Seal Drain Pressure	951,952,953
HPOT Primary Seal Drain Pressure	990
Engine Fuel Inlet Temperature	1021,1017,1018
Engine Oxidizer Inlet Temperature	1058,1054,1056
Fuel Repress Interface Pressure	835
Heat Exchanger Discharge Pressure	34,878

Table 14. Preliminary List of SSME Sensors to Validate

IV.5. Integration of Advanced Models

Several groups are developing advanced models, such as neural networks, which relate data from SSME sensors.[22-25] Since these models appear to perform very well, even during power transients, they are excellent candidates for integration into the validation

network as long as their run-time execution is not too computationally intensive. As NASA provides these models, APD will test and integrate them into the system where needed to provide a more robust validation capability.

IV.6. Software Development and Test

The SDV system will be ported to run on a 486 PC in the TTB blockhouse, where it will receive data in real-time from either live engine firings, or from playbacks of previous tests. APD will be able to run the system and assess its performance remotely from Sacramento via a network connection. The system will have a text-based display and various diagnostic routines to enable its performance to be thoroughly characterized.

V. FY93-95 Programmatics

This section presents an expanded work breakdown structure, and a schedule for completion of the FY93-95 SDV task.

V.1. Expanded Work Breakdown Structure

Subtask 1.0 Project Plan

Aerojet shall deliver one copy-ready document to NASA LeRC for unlimited distribution, summarizing work done to date on real-time sensor data validation tasks under the Development of Life Prediction Capabilities program. The report will cover all important technical results, the viability of using analytical redundancy for SDV, the adequacy of models developed to date for performing SDV on the SSME, and results of validation tests. The PV-Wave and C procedures used to create the models, and the schedules, milestones and expanded work breakdown structure of planned FY93-95 activities will also be delivered to NASA LeRC.

This task will be completed upon acceptance of this report.

Subtask 2.0 Generation of Requirements

Aerojet shall define the detailed requirements for the sensor data validation software. These requirements will include: a final list of sensors to be validated (provided by NASA LeRC); a table describing the accuracy and reliability (Mean-Time Between Failure) of each sensor to be validated; and specification of the maximum acceptable false alarm and missed detection rates for the system. From this information, the following will be derived and specified: the default model residual threshold, the minimum number of relations required per sensor, and the multi-cycle decision strategy. A list of the SSME test firings to be used for software development and validation will be specified by NASA LeRC. These requirements and specifications will be documented and delivered to NASA LeRC for approval.

Subtask 2.1 Document MTBFs for All Sensors to be Validated

APD will identify and document, either via in-person interviews, official documentation, or telecons, the reliability of all SSME sensors on the final list provided by NASA LeRC. Whenever possible the reliabilities shall reflect the *operational* reliabilities of the sensors, that is, hours of SSME hot-fire time between failure (where a failure is any incident which causes the controller to fail to receive an intended engine measurement within the stated accuracy of the sensor involved).

Subtask 2.2 Derivation of SDV Parameters

APD will compute the default model residual threshold, the minimum number of relations required per sensor, and the multi-cycle decision strategy based on sensor reliability data and design goals of 1 false alarm per 1,000 500-second firings and 1 missed detection per 100 500-second firings.

Subtask 2.3 Documentation of Requirements

APD will deliver to NASA a document describing the reliabilities of all sensors to be validated, the values of all SDV parameters derived in Subtask 2.2, and the list of development and validation test firings to be used.

Subtask 2.0 Deliverables

The document produced in Subtask 2.3 will be delivered to NASA LeRC by the completion of this task.

Subtask 3.0 Algorithm Development & Verification

Aerojet shall perform the empirical modeling of SSME test firing data required to develop a robust sensor validation capability as specified in the requirements (e.g., the development of multi-parameter regression models as indicated by the FY92 Sensor Validation task). This modeling will be performed on an as-needed basis using 50 test firings, based on the results of Subtask 2.0 and previous modeling efforts. Advanced analytical redundancy models, such as neural networks, will be included and evaluated as directed by NASA. Aerojet shall integrate characteristic, empirical, and advanced models into a sensor validation network capable of meeting the confidence level specified in the requirements.

A utility program will be written to automate fine-tuning of the residual thresholds to provide the maximum possible sensitivity without an unacceptable false alarm rate. Sensitivity is evaluated by running a simulation in which one sensor value is allowed to drift while all others remain nominal, and noting the point at which the system disqualifies the drifting sensor. The results of these sensitivity tests will be documented. Another utility program will be written and run to compute the biases used on the above 50 datasets. This information will then be used to set the bias limits. Bias limits for each relationship in the sensor validation network shall be reported. Aerojet shall deliver to NASA LeRC a complete description of each model used in the SDV network. Thresholds and bias limits for each model shall be included as well as information regarding the data used for model and threshold development. If different thresholds are used during mainstage and power-level transitions, this will be noted and both will be given.

Subtask 3.1 Interface Requirements for Advanced Models

APD will document the interface requirements for advanced analytical redundancy models, and deliver these requirements to NASA LeRC. Advanced models will have access to sensor values from the current and up to four previous controller cycles, descriptors specifying the current engine state (including power level and lockup status), and clock variables indicating time since start, and time since start of the current engine state. Advanced models supplied by NASA must conform to the interface requirements to be integrated into the final SDV system.

Subtask 3.2 Validation Network Analysis Tool Implementation

A utility program will be developed which reads in a textual representation of a validation network and automatically outputs a report which describes: the degree of coverage for each sensor in the network (i.e., the number of relations it is involved in); the degree of overlap between every pair of sensors in the network (in terms of how many relations they share); the ability of the system to uniquely identify single sensor failures for each sensor in the network; ability to validate all other sensors following a single sensor failure for each sensor in the network; and tabulations of relations by sensor and by cardinality. The reports output by this program will be used to guide the development and refinement of the network.

Subtask 3.3 Threshold Tuning Tool Implementation

A utility program will be developed which tests the false alarm rate of the SDV system, by running it against several nominal test firings and noting the number of times every pair of relations validating a particular sensor fail at the same time. A second utility will be developed to test the sensitivity of the SDV system via drift tests. Results from these programs will be used to automate tuning of the model thresholds. Thresholds will be derived for steady-state and transient operating modes.

Subtask 3.4 Bias Tuning Tool Implementation

A utility program will be developed which derives the bias limits for each model based on analysis of the training test data.

Subtask 3.5 Hard Failure Threshold Tuning Tool Implementation
A utility program will be developed which derives the maximum allowable excursion each redline sensor can make in two consecutive samples under nominal and anomalous operating conditions. This information will be used to set the hard-failure threshold limits.

Subtask 3.6 Data File Preparation
APD will establish a library of the 50 training and 50 test datasets required for the SDV task. All datasets may be stored in a compressed format, and the training datasets may be stored in a reduced format for ease of handling. Software will be implemented to facilitate automatic access of the data by the various utility programs.

Subtask 3.7 SDV Model & Network Development
APD will utilize the utilities described above to develop a robust sensor validation capability as specified. New models will be developed as needed in order to meet the error-rate objectives specified in the requirements.

Subtask 3.8 Test & Integration of Advanced Models
Advanced models supplied by NASA LeRC will be evaluated for possible inclusion into the SDV network. Evaluation shall consist of determining the added coverage to sensors in the network, and the increase in system sensitivity possible without generating false alarms on the training datasets. After reporting these results to NASA LeRC, APD will, at NASA LeRC's direction, integrate the models into the final SDV system.

Subtask 3.9 Documentation
APD will document all models and associated parameters used in the final SDV network. The performance of the final network (sensitivity and false alarm rates) will also be documented and delivered to NASA LeRC.

Subtask 3.0 Deliverables
The document produced in Subtask 3.9, in addition to the documented source code for all utility programs, will be delivered to NASA LeRC by the completion of this task.

Subtask 4.0 Software Development and Test
After receipt of all available documentation describing the PC hardware and software located at NASA MSFC for reading TTBE data in real-time, Aerojet shall produce and deliver to NASA LeRC detailed specifications for the sensor validation software. After the specifications are approved by NASA LeRC, Aerojet shall design, develop, and module test the complete sensor validation software system to be used at the TTB site. The sensor validation system will include a text-based user interface with real-time displays indicating the status of the system and highlighting any failed sensors. The system will also have the capability of archiving data including: samples from selected sensors (e.g, MCC PC); times of sensor failures or near-failures (e.g., one-cycle failures); and selected diagnostic information such as whether a particular model holds or not on each engine cycle. The system will have the capability of being executed and monitored remotely from the contractor's site.

Subtask 4.1 Software Specifications
APD shall produce and deliver to NASA LeRC software specifications for the SDV system to be installed on the PC at the TTB site.

Subtask 4.2 Core Validation System
APD shall design, implement, and module test the core SDV system software on a PC platform.

Subtask 4.3 Data Interface
APD shall design, implement, and module test routines to access data fed from the TTB blockhouse in real time on a PC platform.

Subtask 4.4 User Interface
APD shall design, implement, and module test routines to display (via a text-based display) and log system status and error messages on a PC platform. This software will feature real-time displays indicating the status of the system and highlighting any failed sensors. The software will also have the capability of archiving data including: samples from selected sensors (e.g, MCC PC); times of sensor failures or near-failures (e.g., one-cycle failures); and selected diagnostic information such as whether a particular model holds or not on each engine cycle.

Subtask 4.5 Remote Operation
APD shall design, implement, and module test routines to allow personnel at APD's Sacramento facility and at NASA LeRC to configure, run, monitor, and extract results from the SDV system installed at the TTB facility.

Subtask 4.6 Integration
APD shall integrate all software routines into the final SDV system on a PC platform, compatible with the 486 PC at the TTBE facility.

Subtask 4.0 Deliverables
The software specifications produced in Subtask 4.1, in addition to the documented source code for all software developed, will be delivered to NASA LeRC by the completion of this Subtask.

Subtask 5.0 Verification and Validation
Aerojet shall install and test the sensor validation software on the PC located at the TTB site. All functions of the software shall be tested with TTBE data playbacks. The remote execution function shall be tested to ensure that Aerojet is able to control and evaluate execution of the system from computers at Aerojet Propulsion Division in Sacramento, California.

Aerojet will support the validation of the SDV system through a combination of at least 20 playback live TTBE firings via remote operation from Sacramento.

Subtask 5.1 Installation and Standalone Tests
APD will install the SDV system on the 486 PC at the TTB facility. The software operation will be verified through stand-alone system tests. The remote operation capability will be tested and verified.

Subtask 5.2 TTBE Playback Tests
APD will validate the operation of the SDV through successful on-site monitoring of at least one playback of TTB firing data at the TTB facility.

Subtask 5.3 TTBE Validation Tests
Aerojet will support the validation of the SDV system through a combination of at least 20 playback or live TTBE firings via remote operation from Sacramento.

Subtask 5.0 Deliverables
APD will deliver a document summarizing the results of all live and playback TTBE tests of the SDV system by the completion of this Subtask.

Subtask 6.0 Documentation & Deliverables
Aerojet shall deliver to NASA LeRC final specification, source code and data flow diagrams for the delivered sensor validation system. Aerojet will also deliver a user's manual for the system installed at TTB. A final report documenting the development activities and functionality of the sensor validation system and the results of the validation tests will be prepared and delivered to NASA LeRC. Presentation of these results will be made at NASA LeRC and at NASA MSFC. Recommendations for continued sensor validation system development, including requirements for developing a flight-capable system, will be made and delivered based upon the demonstrated capabilities of the SDV system.

Subtask 6.1 User's Manual
APD shall deliver to NASA LeRC a user's manual for the software installed at the TTB site. The manual shall cover all aspects of the system's operation including remote operation procedures.

Subtask 6.2 Software Documentation
APD shall deliver to NASA LeRC documentation for all developed software, including documented source code, flow charts, and design documents.

Subtask 6.3 Final Report
APD shall deliver to NASA LeRC a final report describing the development activities, results of the TTB validation tests, and suggestions for future work.

Subtask 6.4 Presentations
Presentation of the results documented in the final report will be made at NASA LeRC and at NASA MSFC.

Subtask 6.0 Deliverables
APD shall deliver the documentation produced in Subtasks 6.1 - 6.3 to NASA LeRC by the completion of this Subtask.

Subtask 7.0 (Option 1)
At the discretion of the NASA LeRC Task Manager, the sensor validation system will be extended to monitor approximately 25 of the 97 sensors in Attachment A during the startup transient. The software will be configured so as to provide continuous coverage of these 25 sensors from engine start until shutdown. Parameter models and model thresholds will be provided to Aerojet by NASA LeRC. Aerojet shall evaluate the sensitivity of these models with the same 50 training test firings used for mainstage model development and shall integrate these models into the sensor validation system. The results of the sensitivity test shall be documented and delivered. The same 50 test firings used to validate the mainstage portion of the system will be used to validate the sensor validation system during the start transient. System performance will be documented and delivered as previously described for mainstage.

Subtask 8.0 (Option 2)

At the discretion of the NASA LeRC Task Manager, the sensor validation system will be extended to monitor approximately 25 of the 97 sensors in Attachment A during the startup transient. The software will be configured so as to provide continuous coverage of these 25 sensors from engine start until shutdown. Aerojet shall develop parameter models and model thresholds using the same 50 test firings used for mainstage model development. A complete description of each model used in the SDV network shall be delivered; as well as information regarding the data used for model and threshold development. Aerojet shall evaluate the sensitivity of these models with the same 50 test firings used for mainstage model development and shall integrate these models into the sensor validation system. The results of the sensitivity tests shall be documented and delivered. The same 50 test firings used to validate the mainstage portion of the system will be used to validate the sensor validation system during the start transient. System performance will be documented and delivered as previously described for mainstage.

V.2. Schedule & Milestones

Figure 23 outlines the projected schedule for the FY93-FY95 Real-Time SDV task. Optional subtasks 7.0 and 8.0 were intentionally omitted from the schedule. A decision regarding their implementation should be made by May 1, 1994, at which time tasks 3.8 - 6.4 will be delayed (into FY95) to accommodate.

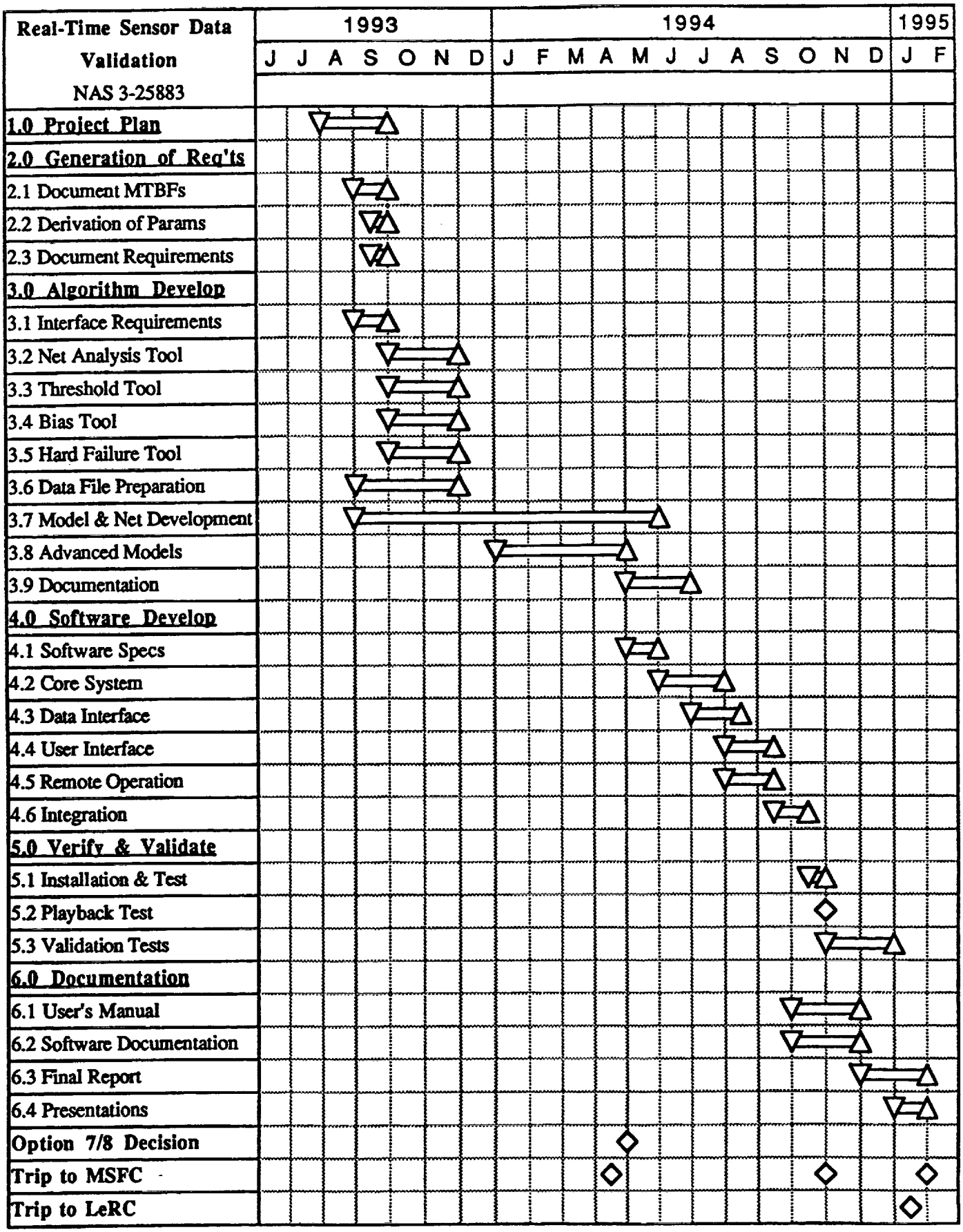

Figure 23. FY93-95 SDV Project Schedule

References

1. *Development of Life Prediction Capabilities for Liquid Propulsion Rocket Engines — Task 3, Sensor Data Validation and Reconstruction, Phase 1: System Architecture Study Final Report*, Aerojet Propulsion Division, Contract NAS 3-25883, March 1991.
2. Smith, C., Broadie, M., and DeHoff, R., *Turbine Engine Fault Detection and Isolation Program: Final Report*, Systems Control Technology, AFWAL-TR-82-2058, August, 1982.
3. Basseville, M. "Detecting Changes in Signals and Systems — A Survey", *Automatica*, Volume 24, 1988.
4. Gumbel, E.J., *Statistics of Extremes*, Columbia University Press, New York, 1958.
5. Lipson and Sheth, *Statistical Design and Analysis of Engineering Experiments*, McGraw-Hill, New York, 1973.
6. Taniguchi, M.H., *Failure Control Techniques for the SSME Phase II: Final Report*, NASA CR-179231, 1987.
7. Dayhoff, J., *Neural Network Architectures*, Van Nostand Reinhold, New York, 1990
8. Lippmann, R.P., "An Introduction to Computing with Neural Nets", *IEEE ASP Magazine*, April, 1987.
9. Wasserman, P.D., *Neural Computing*, Van Nostrand Reinhold, New York, 1990.
10. Frank, P.N., "Fault Diagnosis in Dynamic Systems Using Analytical and Knowledge-based Redundancy—A Survey and Some New Results", *Automatica*, Volume 25, 1989.
11. Merill, W.C., J.C., DeLaat, and W.M. Bruton, "Advanced Detection, Isolation and Accommodation of Sensor Failures — Real-Time Evaluation", NASA Technical Paper 2740, 1987.
12. Isermann, R., "Process Fault Detection Based on Modeling and Estimation Methods — A Survey", *Automatica*, Volume 20, Number 4, 1984.
13. Shortliffe, E., *Computer-Based Medical Consultations: MYCIN*, Elsvier, New York, 1976.
14. Shafer, G., *A Mathematical Theory of Evidence*, Princeton Press, Princeton, New Jersey, 1976.
15. Pearl, J., *Probabilistic Reasoning in Intelligent Systems: Networks of Plausible Inference*, Morgan Kaufmann, San Mateo, California, 1988.
16. Bickmore, T.W., "A Probabilistic Approach to Sensor Data Validation", Paper AIAA 92-3163, AIAA 28th Joint Propulsion Conference, Nashville, Tennessee, 1992.
17. Howard, R., and Matheson, J. "Influence Diagrams", in *Readings on the Principles and Applications of Decision Analysis*, R. Howard and J. Matheson, eds., Strategic Decision Group, Menlo Park, California.
18. Neapolitan, R., *Probabilistic Reasoning in Expert Systems: Theory and Algorithms*, Wiley Interscience, New York, 1990.
19. Walpole, R., and R. Myers, *Probability and Statistics for Engineers and Scientists*, Macmillan, New York, 1978, pp. 238 — 248.
20. De Bruyne, Frank, *Probabilistic Sensor Validation*, Final Project ME290M, Department of Mechanical Engineering, University of California at Berkeley, Fall 1991.
21. *Results from Simulation Laboratory Testing of a Real-Time Sensor Data Validation System*, Aerojet Propulsion Division, 27 March 1992.
22. Meyer, Claudia M., and William A. Maul, *The Application of Neural Networks to the SSME Startup Transient*, Paper #91-2530, 27th Joint Propulsion Conference, June, 1991.
23. Naassan, Kathryn, *Sensor Validation for the Space Shuttle Main Engine Controller*, Master's Thesis, Department of Mechanical Engineering, University of California at Berkeley, December, 1991.

24. Wheeler, Kevin, and Atam Dhawan, *Radial Basis Function Neural Networks Applied to NASA SSME Data*, Technical Report TR154/6/93/ECE, Department of Electrical and Computer Engineering, University of Cincinnati, 1993.
25. Doniere, Timothy, and Atam Dhawan, *LVQ and Backpropagation Neural Networks Applied to NASA SSME Data*, Technical Report RT156/6/93/ECE, Department of Electrical and Computer Engineering, University of Cincinnati, 1993.

Project Plan
for
Real-Time Sensor Data Validation

Attachment 1

Empirical Models Selected for FY92 Modeling Task

PID	Sensor	Eqn Order	Related PID	Related Sensor	Avg Rank	Justification	Results: Fit	Results: Trainable?
260	HPFP SPEED	3	659	HPFP DS T	5.8	Fluid heats as more energy is added.	Med	Good
		1	17	MCC CLNT DS PR	5.9	HPFP SPD -> HPFP DS P -> MCC CLNT DS PR	Med	Good
		1	133	FUEL FLOW	7.3	Speed/flow relation (a first principles relation)	Good	Better
231	HPFT DS TMP CH A	3	42	FPOV ACT POS	8.7	FPOV -> FPB MR -> HPFT DS T	Poor	Good
		3	260	HPFP SPEED	14.4	FPOV -> FPB PC -> HPFT Power -> HPFP SPD	Poor	Med
		3	133	FUEL FLOW	8.4	FPOV -> Turbine Power -> HPFP SPD -> FUEL FLOW (for fixed DS resistance)	Poor	Good
232	HPFT DS TMP CH B	3	42	FPOV ACT POS	12.0	FPOV -> FPB MR -> HPFT DS T	Poor	Good
		3	260	HPFP SPEED	19.0	FPOV -> FPB PC -> HPFT Power -> HPFP SPD	Poor	Med
		3	133	FUEL FLOW	9.0	FPOV -> Turbine Power -> HPFP SPD -> FUEL FLOW (for fixed DS resistance)	Poor	Good
129	MCC PC	1	53	HPFP CLNT LNR P	2.6	CLNT LNR P driven by HPFP DS P which is driven by PC via scheduled fuel flow.	Good	Better
		1	371	MCC HG INJ P	3.2	MCC HG INJ P -> Injector (fixed resistance) -> MCC PC	Good	Better
		1	90	HPOP DS P	4.6	HPOP DS P -> Injector (fixed resistance) -> MCC PC	Good	Not Req
52	HPFP DS P	1	17	MCC CLNT DS PR	2.1	HPFP DS -> Split -> MCC Cooling circuit (fixed resistance) -> MCC CLNT DS P	Med	Good
		1	436	LPFT IN P	2.4	HPFP DS -....(see above)-> MCC CLNT DS P -> line (fixed resistance) -> LPFT IN P	Good	Better
		1	457	HPFP BAL CAV PR	2.4	BAL CAV fed by DS P from pump.	Good	Better
53	HPFP CLNT LNR P	1	129	MCC PC	1.8	MCC PC -> Required Fuel Flow -> FPOV -> HPFP SPD -> HPFP CLNT LNR P	Good	Better
		1	371	MCC HG INJ P	4.3	FPOV affects both HPFP CLNT LNR P and MCC HG INJ P	Good	Better
		3	52	HPFP DS P	6.4	HPFP DS P -> HPFP CLNT LNR P	Med	Good

PID	Sensor	Eqn Order	Related PID	Related Sensor	Avg Rank	Justification	Results: Fit	Results: Trainable?
480	OPB PC	3	334	HPOP DS P	4.1	OPB PC -> HPOTP power -> HPOTP SPD -> HPOP DS P (for fixed DS resistance)	Good	Better
		3	59	PBP DS P	10.6	OPB PC -> HPOTP SPD -> PBP SPD (same shaft) -> PBP DS P (for fixed resistance)	Good	Not Req
58	FPB PC	1	480	OPB PC	2.1	Change in FPB PC causes change in fuel and LOX split between preburners -> OPB PC	Medium	Good
		3	52	HPFP DS P	5.1	FPB PC -> HPFTP SPD -> HPFP DS P (for fixed DS resistance)	Medium	Good
		1	59	PBP DS P	5.2	PBP DS P feeds LOX to FPB PC. Also related through OPB PC.	Medium	Good
42	FPOV ACT POS	1	175	FPOV COM	1.0	FPOV COM -> FPOV POS	Good	Not Req
		1	764	HPFP SPD	5.3	FPOV -> HPFT SPD -> HPFP SPD	Med	Not Req
		3	133	FUEL FLOW	7.7	FPOV -> HPFP SPD -> FLOW (for fixed DS resistance)	Med	Not Req
203	HPFP INLET PR	1	32	LPFP SPD	4.1	LPFP SPD -> LPFP DS P (for fixed DS resistance) -> HPFP IN P	Poor	(Bi-Modal indicates 3rd parameter may be needed.)
		1	93	PBP DS T	5.3		Poor	
		1	764	HPFP SPD	8.9	Change in HPFP IN P will cause change in HPFP SPD to maintain constant flow.	Poor	
1212	OX FLOW	1	334	HPOP DS P	2.1	HPOP pumping to fixed DS resistance, so change in DS P effected by change in flow.	Good	Not Req
		1	129	MCC PC	5.8	Related to HPOP DS P by fixed resistance.	Good	Not Req
		1	480	OPB PC	9.1	OPB PC -> HPOTP SPD -> LOX FLOW	Good	Not Req
133	FUEL FLOW	3	764	HPFP SPD	3.7	Pump flow and speed relation.	Good	Not Req
		1	371	MCC HG INJ P	5.0	Majority of fuel ends up flowing as hot gas into MCC across fixed resistance injector.	Good	Not Req
		3	17	MCC CLNT DS P	6.8	FUEL FLOW -> Fork -> MCC Cooling circuit (fixed resistance) -> MCC CLNT DS P	Med	Good

PID	Sensor	Eqn Order	Related PID	Related Sensor	Avg Rank	Justification	Results: Fit	Results: Trainable?
17	MCC CLNT DS P	1	436	LPFT IN P	1.8	Related by direct line (fixed resistance).	Good	Better
		1	52	HPFP DS P	1.9	HPFP DS P -> fork -> MCC cooling circuit (fixed resistance) -> MCC CLNT DS P	Med	Good
		1	764	HPFP SPD	17.8	HPFP SPD -> HPFP DS P -> MCC CLNT DS P	Med	Good
436	LPFT IN P	1	17	MCC CLNT DS P	2.0	Related by direct line.	Med	Good
		1	52	HPFP DS P	2.9	HPFP DS P -> fork -> MCC cooling circuit -> LPFT IN P	Med	Good
		1	764	HPFP SPD	17.8	HPFP SPD -> HPFP DS P (for fixed DS resistance) -> LPFT IN P (see above)	Med	Good
32	LPFP SPD	3	764	HPFP SPD	2.8	HPFP SPD -> HPFP DS P -> fork -> MCC cooling -> LPFT -> LPFP SPD. Also, change in LPFP SPD must be compensated by HPFP.	Med	Good
		3	722	FUEL FLOW	8.3	Pump speed flow relation.	Med	Good
		3	436	LPFT IN P	13.7	Turbine head/speed relation.	Med	Good
30	LPOP SPD	1	129	MCC PC	3.2	LPOP SPD driven by HPOP DS P, which is a fixed resistance away from MCC PC.	Med	Good
		1	59	PBP DS P	8.1	LPOP SPD closely linked to HPOP SPD which is connected to PBP.	Med	Good
		1	1212	OX FLOW	10.0	Pump speed/flow relation.	Med	Good
233	HPOT DS T	1	30	LPOP SPD	3.1	LPOP SPD closely linked to HPOP SPD, which is driven by OPB PC, which drives this.	Poor	(Bi-Modal indicates 3rd parameter may be needed.)
		1	480	OPB PC	8.3	LPOP SPD closely linked to HPOP SPD which is driven by OPB PC.	Poor	
		3	40	OPOV ACT POS	5.1	OPOV controls OPB PC and temp, which drives HPOT DS T.	Poor	
234	HPOT DS T	1	30	LPOP SPD	3.8	LPOP SPD closely linked to HPOP SPD, which is driven by OPB PC, which drives this.	Poor	(Bi-Modal indicates 3rd parameter may be needed.)
		1	480	OPB PC	7.6	LPOP SPD closely linked to HPOP SPD which is driven by OPB PC.	Poor	
		3	40	OPOV ACT POS	6.1	OPOV controls OPB PC and temp, which drives HPOT DS T.	Poor	

PID	Sensor	Eqn Order	Related PID	Related Sensor	Avg Rank	Justification	Results: Fit	Results: Trainable?
21	MCC LOX DOM T	1	93	PBP DS T	1.0	HPOP IN -> both DOME and PBP DS	Good	Not Req
		3	30	LPOP SPD	4.3	LPOP SPD and HPOP SPD closely linked. HPOP SPD increase adds more energy to LOX	Med	Not Req
		3	40	OPOV ACT POS	4.8	OPOV drives HPOP SPD which adds energy to LOX.	Med	Not Req
176	OPOV COMMAND	3	480	OPB PC	18.0	OPOV COM -> OPOV POS	Med	Not Req
		3	30	LPOP SPD	5.8	LPOP SPD and HPOP SPD closely linked. OPOV drives HPOTP speed.	Med	Not Req
		3	129	MCC PC	8.6	PC control loop (PC -> OPOV).	Med	Not Req
40	OPOV ACT POS	3	30	LPOP SPD	2.2	LPOP SPD and HPOP SPD closely linked. OPOV drives HPOTP speed.	Med	Not Req
		3	129	MCC PC	8.6	PC control loop (PC -> OPOV).	Med	Not Req
		3	480	OPB PC	17.1	OPOV drives OPB PC.	Med	Not Req
18	MCC CLNT DS T	1	225	HPFP INLET T	1.8	HPFP IN -> HPFP -> fork -> MCC cool circuit -> MCC CLNT DS T	Poor	
		1	1017	FL FAC FM DS T	5.3	FAC -> LPFP -> HPFP IN -> HPFP -> fork -> MCC cool circuit -> MCC CLNT DS T	Poor	
		1	21	MCC LOX DOM T	5.6	MCC LOX DOM T & MCC CLNT DS T adjacent & both affected by MCC temp.	Poor	
209	HPOP IN P	1	327	HPOP BAL CAV P	7.4		UNUSABLE	(Bi-Modal indicates 3rd parameter may be needed.)
		1	858	ENG OX IN P	11.0	LPOP provides constant deltaP step between ENG OX IN P and HPOP IN P.	UNUSABLE	
		3	234	HPOT DS T	13.7	HPOT DS T measure of power of HPOTP, which drives LPOP -> HPOP IN P.	UNUSABLE	

PID	Sensor	Eqn Order	Related PID	Related Sensor	Avg Rank	Justification	Results Fit	Results Trainable?
93	PBP DS T	1	21	MCC LOX DOM T	1.0	HPOP IN -> both DOME and PBP DS	Good	Not Req
		3	40	OPOV ACT POS	5.7	OPOV drives HPOTP & PBP speeds, which add more energy to LOX at PBP DS.	Med	Not Req
		3	30	LPOP SPD	3.1	LPOP SPD and HPOP SPD closely related. Speed can add more energy to LOX.	Med	Good
1951	MCC LINER CAV P	1	990	HPOT PR SL DR P	1.3		UNUSABLE	
		1	91	HPOT S/C PR	1.8		UNUSABLE	
		1	819	ENG FL IN P	2.9		UNUSABLE	
90	HPOP DS P	1	129	MCC PC	4.0	Separated by fixed resistance across injector.	Good	Not Req
		1	480	OPB PC	6.7	OPB drives HPOTP speed -> pump speed/head relation.	Good	Better
59	PBP DS P	3	480	OPB PC	1.3	OPB drives HPOTP & PBP speed -> pump speed/head relation.	Good	Not Req
		3	90	HPOP DS P	3.4	HPOTP speed drives both DS Ps via pump speed/head relation.	Good	Not Req
659	HPFP DS T	3	764	HPFP SPD	1.2	More speed adds more energy to fuel.	Med	Good
		1	722	ENG FL FLOW	9.2	DS T measure of power of HPFTP, which drives amount of fuel flow.	Med	Good
		1	52	HPFP DS P	8.6	As pump speed increase, DS P (via fixed DS resistance) and temp (via more energy) go up.	Med	Good
211	HPOP ISP P	1	231	HPFT DS T A	5.1		UNUSABLE	
		1	232	HPFT DS T B	6.9		UNUSABLE	
		1	175	FPOV COM	8.8		UNUSABLE	

PID	Sensor	Eqn Order	Related PID	Related Sensor	Avg Rank	Justification	Results Fit	Results Trainable?
91	HPOT S/C P	1	990	HPOT PR SL DR P	1.0		Poor	Med
		1	1951	MCC LINER CAV P	2.1		Poor	Not Req
		1	211	HPOP ISP P	14.7		UNUSABLE	
225	HPFP IN T	1	1017	FL FAC FM DS T	2.4	Fuel: FAC -> ENG IN -> LPFP -> HPFP IN T	UNUSABLE	
		1	1021	ENG FL IN T	4.4	Fuel: FAC -> ENG IN -> LPFP -> HPFP IN T	UNUSABLE	
		1	18	MCC CLNT DS T	5.4	HPFP IN -> HPFP DS -> fork -> MCC cool circuit -> MCC CLNT DS T	UNUSABLE	
		3	659	HPFP DS T	8.4	HPFP IN -> HPFP -> HPFP DS		
327	HPOP BALCAV P	1	129	MCC PC	3.6	BALCAV fed by HPOP DS P, which is a fixed resistance away from MCC PC.	Med	Good
		3	334	HPOP DS P	4.1	BALCAV fed by HPOP DS P.	Med	Good
		3	480	OPB PC	15.9	BALCAV fed by HPOP DS P which is driven by HPOTP SPD which is driven by OPB PC.	Med	Good
457	HPFP BAL CAV P	1	52	HPFP DS P	1.1	BALCAV fed by HPFP DS P.	Good	Better
		3	436	LPFT IN P	3.1	BALCAV fed by HPFP DS P which indirectly drives LPFT IN P.	Med	Good
		3	17	MCC CLNT DS P	7.9	BALCAV fed by HPFP DS P which drives MCC CLNT DS P.	Med	Good
650	HPFP CLNT LN T	1	764	HPFP SPD	12.2	HPFP SPD -> HPFP DS T -> HPFP CLNT T	UNUSABLE	
		1	659	HPFP DS T	12.3	HPFP DS feeds HPFP CLNT LN.	UNUSABLE	
		1	232	HPFT DS T B	13.0	HPFT DS T measure of HPFTP power -> HPFTP SPD -> HPFP CLNT LN T	UNUSABLE	

PID	Sensor	Eqn Order	Related PID	Related Sensor	Avg Rank	Justification	Results Fit	Results Trainable?
819	ENG FL IN P	3	231	HPFT DS T	11.9	Change in FL IN P cause HPFTP to change power which is reflected in HPFT DS T.	UNUSABLE	(Bi-Modal indicates
		1	1951	MCC LINER CAV P	2.0		UNUSABLE	3rd parameter
		1	436	LPFT IN P	12.4	Change in FL IN P cause HPFTP to change power which is reflected in HPFP DS P.	UNUSABLE	may be needed.)
858	ENG OX IN P	1	209	HPOP IN P	1.1	Separated by LPOP which provides constant delta-P.	UNUSABLE	(Bi-Modal indicates
		1	951	HPOP PR SL DR P	9.6	Fed by HPOP DS P which is driven by HPOP IN P which is driven by ENG OX IN P.	UNUSABLE	3rd parameter
		1	40	OPOV ACT POS	12.4	Change in OX IN P results in change HPOTP power which is effected via OPOV.	UNUSABLE	may be needed.)
951	HPOP PR SL DR P	1	211	HPOP ISP PR	13.7		UNUSABLE	
		1	209	HPOP IN P	14.9	HPOP PR SL DR P is fed by HPOP DS P which is driven by HPOP IN P.	UNUSABLE	
		1	1951	MCC LINER CAV P	19.9		UNUSABLE	
990	HPOT PR SL DR P	1	91	HPOT S/C PR	1.0		Poor	Med
		1	1951	MCC LINER CAV P	2.1		Poor	Not Req
		1	1190	HPOT PRSL DR T	3.4		UNUSABLE	
1021	ENG FL IN T	1	225	HPFP IN T	3.9	Separated only by LPFP.	UNUSABLE	
		1	18	MCC CLNT DS T	5.8	MCC CLNT DS T function of ENG FL IN T, energy added by HPFP and MCC temp.	UNUSABLE	
		1	231	HPFT DS T A	16.3	Fuel press or vent requires change in HPOTP power, which effects HPFT DS T.	UNUSABLE	
1017	FL FAC FM DS T	1	225	HPFP IN T	3.4	Separated only by LPFP.	UNUSABLE	
		1	18	MCC CLNT DS T	5.7	MCC CLNT DS T function of ENG FL IN T, energy added by HPFP and MCC temp.	UNUSABLE	
		1	231	HPFT DS T A	8.8	Fuel press or vent requires change in HPOTP power, which effects HPFT DS T.	UNUSABLE	

PID	Sensor	Eqn Order	Related PID	Related Sensor	Avg Rank	Justification	Results: Fit	Results: Trainable?
1058	ENG OX IN T	1	21	MCC LOX DOM T	7.2	LOX DOM T a function of ENG OX IN T and energy added by HPOP.	UNUSABLE	
		1	93	PBP DS T	9.0	Separated only by LPOP and PBP.	UNUSABLE	
		3	1190	HPOT PRSL DR T	9.1		UNUSABLE	
1054	OX FAC FM DS T	1	21	MCC LOX DOM T	7.4	LOX DOM T a function of ENG OX IN T and energy added by HPOP.	UNUSABLE	
		1	93	PBP DS T	9.1	Separated only by LPOP and PBP.	UNUSABLE	
		3	1190	HPOT PRSL DR T	9.4		UNUSABLE	
1188	HPOT SECSL DR T	3	1951	MCC LINER CAV P	1.6		UNUSABLE	
		1	21	MCC LOX DOM T	4.8		UNUSABLE	
		3	990	HPOT PR SL DR P	7.0		UNUSABLE	
1190	HPOT PRSL DR T	1	233	HPOT DS T A	4.1	Adjacent to turbine, so influenced strongly by turbine temps.	UNUSABLE	
		1	990	HPOT PR SL DR P		Redundant.	UNUSABLE	
		3	93	PBP DS T	15.4		UNUSABLE	
835	FL PRESS INT P	1	722	ENG FL FLOW	5.7	ENG FL FLOW related to pump speed, which is related to turbine speed, which defines delta-P across LPFP, which drives FL PRESS.	Med	Good
		1	436	LPFT IN P	6.7	Separated only by LPFT.	Med	Good
		1	17	MCC CLNT DS P	8.0	Separated only by line between MCC and LPFT, and LPFT.	Med	Good

PID	Sensor	Eqn Order	Related PID	Related Sensor	Avg Rank	Justification	Results: Fit	Results: Trainable?
764	HPFP SPD	3	659	HPFP DS T	6.1	Higher speed adds more energy to fuel.	Med	Good
		1	17	MCC CLNT DS P	6.2	HPFP SPD related to HPFP DS P which drives MCC CLNT DS P.	Med	Good
		1	133	FUEL FLOW	7.9	First principles pump relation.	Good	Better
175	FPOV COM	1	42	FPOV ACT POS	1.0	Command and actual should be same.	Good	Not Req
		3	764	HPFP SPD	3.4	FPOV drives HPOT which drives HPFP SPD.	Med	Not Req
		1	133	FUEL FLOW	11.4	FPOV drives HPOT which drives HPFP SPD which drives fuel flow (for fixed DS res).	Med	Not Req
722	ENG FL FLOW	3	764	HPFP SPD	1.6	First principles pump relation.	Good	Not Req
		1	371	MCC HG INJ P	2.7	Line resistance across fixed-resistance injector (majority of fuel winds up as MCC HG).	Good	Not Req
		3	17	MCC CLNT DS P	7.4	HPFTP speed drives HPFP DS which drives MCC cooling circuit DS P.	Med	Good
1205	FAC FL FLOW	1	371	MCC HG INJ P	3.1	Line resistance across fixed-resistance injector (majority of fuel winds up as MCC HG).	Good	Not Req
		3	764	HPFP SPD	3.2	First principles pump relation.	Med	Good
		3	17	MCC CLNT DS P	9.9	HPFTP speed drives HPFP DS which drives MCC cooling circuit DS P.	Med	Not Req
371	MCC HG INJ P	1	129	MCC PC	3.0	Separated by fixed-resistance injector.	Good	Not Req
		1	722	ENG FL FLOW	3.3	Line resistance across fixed-resistance injector (majority of fuel winds up as MCC HG).	Good	Not Req
		1	53	HPFP CLNT LNR P	5.4	???	Good	Not Req

Project Plan
for
Real-Time Sensor Data Validation

Attachment 2

Empirical Model Coefficients Averaged Over Training Datasets for FY92 Modeling Task

.Binary relation, Linear fit coefficients. (Page 1 of 4)

PidY	PidX	R.Mean	R.Sigma	C0	C1
260	659	-1.98E+01	6.19E+02	-6.2050E+03	4.3120E+02
260	17	-2.07E+01	4.82E+02	1.3118E+04	4.9001E+00
260	133	-4.93E+00	3.13E+02	1.3082E+04	1.3620E+00
231	42	-3.00E+00	6.30E+01	6.1976E+02	1.3366E+01
231	260	-2.34E+00	6.54E+01	9.7958E+02	2.0530E-02
231	133	-2.11E+00	6.52E+01	1.2568E+03	2.7374E-02
232	42	-3.04E+00	4.63E+01	2.0918E+02	1.8859E+01
232	260	-3.12E+00	4.89E+01	6.8588E+02	2.9914E-02
232	133	-2.82E+00	5.03E+01	1.0806E+03	4.0493E-02
129	53	-3.91E-01	1.91E+01	8.6613E+01	8.8521E-01
129	371	-6.28E-01	1.53E+01	1.0620E+02	9.0918E-01
129	90	-4.35E-01	1.35E+01	3.7498E+02	6.7443E-01
52	17	-1.92E+00	1.10E+02	-1.5935E+02	1.3971E+00
52	436	2.57E-01	7.43E+01	-1.6568E+02	1.4161E+00
52	457	1.12E+00	7.24E+01	-8.1476E+01	1.2889E+00
53	129	2.86E-01	2.15E+01	-9.6376E+01	1.1292E+00
53	371	-3.68E-01	2.47E+01	2.3347E+01	1.0267E+00
53	52	-1.06E+00	4.92E+01	1.7741E+01	5.5873E-01
480	334	1.83E+00	3.66E+01	-4.4059E+02	1.3893E+00
480	328	1.83E+00	3.66E+01	-4.4059E+02	1.3893E+00
480	59	1.02E+00	4.27E+01	-2.0223E+02	7.3421E-01
58	480	-1.60E+00	8.25E+01	1.6447E+02	9.5497E-01
58	59	-2.66E-01	8.74E+01	-3.1200E+01	7.0147E-01
58	52	-8.55E-01	1.14E+02	-7.9255E+02	9.7320E-01
42	175	-1.96E-03	1.38E-01	-1.1274E+00	1.0204E+00
42	764	2.09E-02	1.08E+00	2.4777E+01	1.6021E-03
42	133	1.10E-02	1.27E+00	4.5958E+01	2.1634E-03
203	32	1.73E-01	7.66E+00	7.9614E+01	9.4303E-03
203	93	-3.94E-01	9.64E+00	2.4492E+00	1.0891E+00
203	764	-2.27E-01	9.35E+00	1.2645E+02	2.8747E-03
1212	334	1.70E-01	3.56E+01	7.1748E+02	1.2758E+00
1212	129	9.52E-01	4.73E+01	1.3358E+01	1.8906E+00
1212	480	-1.69E+00	5.29E+01	1.1263E+03	9.1746E-01
133	371	-4.87E+00	1.18E+02	4.8923E+02	4.7242E+00
133	17	-1.10E+01	3.15E+02	4.4807E+01	3.5933E+00
133	764	1.99E+00	1.86E+02	-9.4030E+03	7.2917E-01
17	436	1.35E+00	3.74E+01	-2.3813E+00	1.0153E+00
17	52	1.32E-01	7.46E+01	1.1716E+02	7.1756E-01
17	764	1.40E+00	7.99E+01	-2.6240E+03	2.0312E-01
436	17	-1.42E+00	4.41E+01	5.9125E+00	9.8618E-01
436	52	-1.01E+00	5.24E+01	1.2050E+02	7.0568E-01
436	764	1.44E+00	6.99E+01	-2.5855E+03	2.0010E-01
32	764	-1.12E+01	2.29E+02	4.4859E+03	3.1815E-01
32	722	-1.04E+01	2.79E+02	8.6624E+03	4.3172E-01
32	436	-1.44E+01	2.20E+02	8.6901E+03	1.5679E+00
30	129	-1.99E+00	6.71E+01	1.7876E+03	1.0905E+00
30	59	-2.89E+00	6.40E+01	2.3223E+03	3.8856E-01
30	1212	-2.40E+00	6.81E+01	1.7883E+03	5.7527E-01

.Binary relation, Linear fit coefficients. (Page 2 of 4)

PidY	PidX	R.Mean	R.Sigma	C0	C1
233	30	1.33E+00	5.10E+01	-1.4766E+01	2.6332E-01
233	480	-1.05E+00	5.96E+01	6.2909E+02	1.3880E-01
233	40	2.81E-01	4.97E+01	-2.4230E+02	2.3993E+01
234	30	1.12E+00	4.64E+01	-6.9329E+01	2.7362E-01
234	480	-7.10E-01	5.33E+01	5.9808E+02	1.4443E-01
234	40	2.57E-01	4.24E+01	-3.0831E+02	2.4967E+01
24	129	-5.71E+01	1.57E+03	-4.8986E+01	6.2460E-01
24	53	-5.83E+01	1.58E+03	-8.7063E-01	5.5505E-01
24	722	-5.47E+01	1.57E+03	-4.5360E+01	1.2042E-01
21	93	-1.75E-02	8.46E-01	3.1736E+01	7.8683E-01
21	30	1.69E-02	2.56E+00	1.2681E+02	1.2964E-02
21	40	-1.77E-02	2.47E+00	1.1417E+02	1.2033E+00
176	30	2.44E-02	1.39E+00	1.1929E+01	1.0457E-02
176	480	-8.59E-03	1.37E+00	3.7404E+01	5.5188E-03
176	129	-1.21E-03	1.45E+00	3.0733E+01	1.1367E-02
40	30	1.88E-02	1.39E+00	1.0920E+01	1.0693E-02
40	129	-9.07E-03	1.47E+00	3.0123E+01	1.1632E-02
40	480	-1.68E-02	1.38E+00	3.6940E+01	5.6492E-03
18	225	1.91E-01	1.84E+01	-3.6711E+00	1.0352E+01
18	1017	5.43E-02	2.03E+01	2.3863E+01	1.1029E+01
18	21	4.18E-01	1.97E+01	2.3024E+02	1.0653E+00
209	327	-9.40E-02	2.60E+01	1.9806E+02	5.0211E-02
209	858	1.68E-01	2.43E+01	2.7952E+02	7.6803E-01
209	234	-2.06E+00	3.09E+01	2.3312E+02	8.6073E-02
93	21	5.70E-03	1.08E+00	-3.7547E+01	1.2565E+00
93	40	-1.36E-02	2.71E+00	1.0284E+02	1.5595E+00
93	30	4.56E-02	2.62E+00	1.1870E+02	1.6902E-02
1951	990	-2.28E-02	6.71E-01	-1.1034E+01	1.4558E-01
1951	91	1.45E-02	7.56E-01	-1.3815E+01	3.2514E-01
1951	819	-1.46E-02	7.88E-01	-1.1119E+01	1.3328E-01
90	328	1.08E-02	1.38E+01	4.0283E-01	9.9949E-01
90	129	5.78E-01	1.99E+01	-5.5293E+02	1.4817E+00
90	480	-1.51E+00	2.77E+01	3.1915E+02	7.1907E-01
59	480	-1.88E+00	5.83E+01	2.8383E+02	1.3604E+00
59	90	5.93E-01	7.45E+01	-3.1455E+02	1.8905E+00
59	328	7.53E-01	7.27E+01	-3.1504E+02	1.8899E+00
659	764	1.69E-02	1.40E+00	1.4823E+01	2.3099E-03
659	722	1.10E-02	1.69E+00	4.4922E+01	3.1499E-03
659	52	-2.42E-02	1.96E+00	4.6531E+01	8.0671E-03
211	231	-1.97E-01	1.41E+01	-4.7988E+01	1.8014E-01
211	232	1.41E-01	1.35E+01	4.9194E+01	1.2016E-01
211	175	-7.03E-01	1.45E+01	7.4020E+01	2.2898E+00
91	990	-2.26E-02	1.02E+00	8.6122E+00	4.3815E-01
91	1951	1.35E-01	1.96E+00	3.5978E+01	2.4138E+00
91	211	1.08E-01	2.19E+00	3.1310E+01	-7.4056E-02
225	1017	-5.15E-04	2.83E-01	1.2148E+00	1.1038E+00
225	1021	6.28E-03	3.61E-01	3.4968E+00	1.0409E+00
225	18	-1.79E-01	1.32E+00	9.9661E+00	7.4869E-02
327	129	2.06E+00	8.70E+01	-1.9390E+02	1.0446E+00
327	334	1.33E+00	8.89E+01	1.9670E+02	7.0458E-01
327	480	3.63E-01	9.37E+01	4.2494E+02	5.0615E-01

.Binary relation, Linear fit coefficients. (Page 3 of 4)

PidY	PidX	R.Mean	R.Sigma	C0	C1
457	52	-1.86E+00	5.62E+01	6.6748E+01	7.7542E-01
457	436	-1.22E+00	7.00E+01	-6.1733E+01	1.0980E+00
457	17	-3.15E+00	1.03E+02	-5.5721E+01	1.0830E+00
650	764	-1.25E+00	3.07E+01	1.8714E+02	3.1693E-03
650	659	-8.56E-01	2.98E+01	1.6523E+02	1.3845E+00
650	232	5.69E-01	3.01E+01	1.0854E+02	1.0850E-01
819	436	9.10E-02	4.55E+00	3.1860E+01	-4.9651E-03
819	231	3.39E-02	5.38E+00	8.7912E+01	-4.5901E-02
819	1951	1.28E-01	4.46E+00	5.5747E+01	4.6345E+00
858	209	1.46E+00	2.27E+01	-1.6778E+02	7.2514E-01
858	951	1.94E+03	1.98E+03	-7.9473E+01	-2.6943E+02
858	40	-4.27E-01	3.06E+01	1.8579E+02	-1.5994E+00
951	211	-1.69E-02	7.36E+00	5.5833E+00	4.0491E-03
951	209	8.33E-03	7.36E+00	6.5431E+00	1.1546E-04
951	1951	-3.97E-03	7.36E+00	6.0043E+00	-6.1257E-02
990	91	5.61E-02	2.34E+00	-1.8480E+01	2.2000E+00
990	1951	2.15E-01	4.05E+00	6.3054E+01	5.5542E+00
990	1190	-5.88E-01	6.37E+00	-7.6084E+01	9.5423E-02
1021	225	1.11E-02	3.06E-01	2.8014E+00	8.1476E-01
1021	18	-1.20E-01	1.19E+00	1.2327E+01	5.7721E-02
1021	231	-5.87E-02	6.77E-01	3.0702E+01	3.9803E-03
1017	225	8.70E-03	2.38E-01	1.7168E+00	8.3921E-01
1017	18	-1.31E-01	1.23E+00	1.0777E+01	6.1194E-02
1017	231	-5.58E-02	6.64E-01	2.8566E+01	5.2249E-03
1058	21	2.43E-02	2.38E+00	1.1720E+02	2.5016E-01
1058	93	4.57E-03	2.52E+00	1.3049E+02	1.7063E-01
1058	1190	1.38E-01	2.78E+00	1.4905E+02	1.7657E-02
1054	21	2.14E-02	2.36E+00	1.1701E+02	2.4935E-01
1054	93	1.29E-03	2.50E+00	1.3023E+02	1.7014E-01
1054	1190	1.36E-01	2.77E+00	1.4904E+02	1.7275E-02
1188	21	-1.37E-01	3.35E+01	1.8923E+02	3.0263E+00
1188	1951	-1.16E+00	3.86E+01	7.3597E+02	-3.6771E+00
1188	990	-3.50E-01	3.74E+01	7.6758E+02	3.2966E-01
1190	233	5.03E-01	5.49E+01	5.4257E+02	2.7825E-01
1190	990	1.07E+00	5.75E+01	8.5214E+02	5.4148E+00
1190	93	-8.27E-01	5.77E+01	1.3575E+02	3.7909E+00
835	722	-1.78E+00	6.36E+01	2.8361E+01	2.0371E-01
835	436	-3.83E+00	6.90E+01	4.2789E+01	7.3953E-01
835	17	-5.71E+00	8.47E+01	4.7778E+01	7.2934E-01
764	659	-1.93E+01	6.05E+02	-6.2031E+03	4.3075E+02
764	17	-1.98E+01	4.49E+02	1.3093E+04	4.8965E+00
764	133	-4.06E+00	2.56E+02	1.3057E+04	1.3609E+00
175	42	1.35E-03	1.35E-01	1.1699E+00	9.7916E-01
175	764	2.34E-02	1.08E+00	2.5494E+01	1.5668E-03
175	133	1.34E-02	1.28E+00	4.6224E+01	2.1146E-03
722	371	-7.66E+00	1.10E+02	5.5275E+02	4.7008E+00
722	764	-6.05E-01	1.86E+02	-9.2833E+03	7.2534E-01
722	17	-1.47E+01	3.26E+02	1.1569E+02	3.5746E+00
1205	371	-5.80E+00	1.39E+02	3.8688E+02	4.6454E+00
1205	17	-1.22E+01	3.11E+02	-4.2931E+01	3.5318E+00
1205	764	1.01E+00	1.97E+02	-9.3276E+03	7.1663E-01

.Binary relation, Linear fit coefficients. (Page 4 of 4)

PidY	PidX	R.Mean	R.Sigma	C0	C1
371	129	5.36E-01	1.68E+01	-1.1456E+02	1.0992E+00
371	722	1.30E+00	2.33E+01	-1.1577E+02	2.1263E-01
371	53	1.51E-01	2.40E+01	-1.9540E+01	9.7305E-01
328	334	-1.31E-07	4.00E-06	8.1380E-05	1.0000E+00
328	480	-1.49E+00	2.63E+01	3.1971E+02	7.1927E-01
328	129	5.73E-01	2.41E+01	-5.5152E+02	1.4818E+00
334	328	-1.31E-07	4.00E-06	8.1380E-05	1.0000E+00
334	480	-1.49E+00	2.63E+01	3.1971E+02	7.1927E-01
334	129	5.73E-01	2.41E+01	-5.5152E+02	1.4818E+00

Binary relation, cubic fit coefficients. (Page 1 of 3)

PidY	PidX	R.Mean	R.Sigma	C0	C1	C2	C3
260	659	1.35E+01	5.31E+02	5.5961E+04	-2.0192E+03	3.1481E+01	-1.3229E-01
260	17	-2.52E+01	5.13E+02	-2.8711E+04	3.8019E+01	-8.5447E-03	7.2206E-07
260	133	-1.79E+01	2.82E+02	-4.3776E+04	1.4238E+01	-9.5189E-04	2.3059E-08
231	42	-3.02E+00	6.12E+01	-2.3029E+03	1.2953E+02	-1.5203E+00	6.5610E-03
231	260	-1.56E+00	6.24E+01	-4.5641E+03	5.5106E-01	-1.6766E-05	1.7516E-10
231	133	-2.33E+00	6.07E+01	-5.9086E+03	1.6615E+00	-1.2170E-04	2.9694E-09
232	42	-3.18E+00	4.49E+01	1.6693E+03	-6.9259E+01	1.5663E+00	-8.6506E-03
232	260	-1.14E+00	4.60E+01	-2.4493E+03	3.0338E-01	-7.7762E-06	7.2032E-11
232	133	-2.05E+00	4.48E+01	-5.8292E+03	1.5998E+00	-1.1483E-04	2.7702E-09
129	53	-2.18E-01	1.87E+01	7.8807E+01	8.3572E-01	3.8660E-05	-6.8499E-09
129	371	-8.46E-01	1.46E+01	-2.0499E+02	1.2146E+00	-9.4945E-05	9.4072E-09
129	90	-5.46E-02	1.12E+01	-5.0735E+02	1.4235E+00	-2.0321E-04	1.7799E-08
52	17	-4.51E+00	1.14E+02	1.0966E+02	1.3020E+00	-9.0520E-06	3.7503E-09
52	436	-1.70E+00	7.69E+01	-5.7425E+02	1.8940E+00	-1.6753E-04	1.8134E-08
52	457	3.84E+00	6.23E+01	2.0724E+03	-5.2601E-01	4.9638E-04	-4.4053E-08
53	129	1.76E-01	2.16E+01	1.0433E+02	9.5281E-01	4.3807E-05	-2.5443E-09
53	371	-8.22E-01	2.49E+01	-1.6735E+02	1.2470E+00	-8.2800E-05	1.0171E-08
53	52	1.10E+00	4.16E+01	2.3596E+03	-1.0039E+00	3.3798E-04	-2.3692E-08
480	334	1.10E+00	3.30E+01	5.1002E+02	6.5828E-01	1.7164E-04	-1.2169E-08
480	328	1.10E+00	3.30E+01	5.1002E+02	6.5828E-01	1.7164E-04	-1.2169E-08
480	59	9.86E-01	4.21E+01	7.3474E+02	3.1814E-01	5.7192E-05	-2.4476E-09
58	480	-4.86E+00	8.29E+02	3.3921E+01	1.0747E+00	-3.3212E-05	2.8986E-09
58	59	-3.04E+00	8.94E+01	5.3222E+02	4.9761E-01	1.9042E-05	-2.4454E-10
58	52	-1.33E+00	1.01E+02	6.8227E+03	-3.6992E+00	9.3629E-04	-6.1404E-08
42	175	3.55E-04	1.33E-01	1.1290E+01	4.7383E-01	7.8942E-03	-3.7508E-05
42	764	-2.29E-02	9.49E-01	-1.9457E+02	2.4518E-02	-7.8676E-07	8.8840E-12
42	133	-7.68E-02	1.19E+00	-1.7709E+02	5.4224E-02	-3.9676E-06	9.8951E-11
203	32	-4.97E-01	7.23E+00	-5.1272E+02	1.4700E-01	-1.0445E-05	2.6027E-10
203	93	4.29E-03	9.68E+00	5.3741E+02	-9.4565E+00	6.5840E-02	-1.3233E-04
203	764	-1.22E-01	9.12E+00	-5.6975E+02	7.0941E-02	-2.1963E-06	2.3413E-11
1212	334	-3.76E-01	3.54E+01	-6.4374E+02	2.4473E+00	-3.2341E-04	2.8947E-08
1212	129	9.71E-01	4.69E+01	1.1416E+03	5.8040E-01	4.9687E-04	-6.1768E-08
1212	480	-6.29E-01	4.85E+01	-4.7243E+02	1.9458E+00	-2.0542E-04	1.2870E-08
133	371	-6.24E+00	1.19E+02	-4.6847E+02	5.8328E+00	-4.1958E-04	5.1964E-08
133	17	2.33E+00	2.66E+02	1.0984E+04	-5.9509E+00	2.7134E-03	-2.5149E-07
133	764	1.56E+00	1.08E+02	4.1221E+04	-4.1270E+00	1.5376E-04	-1.6092E-09
17	436	1.15E+00	3.72E+01	-3.6763E+02	1.3238E+00	-8.4596E-05	7.5718E-09
17	52	1.89E+00	7.51E+01	2.9022E+02	5.3860E-01	5.0398E-05	-4.2065E-09
17	764	2.40E+00	7.69E+01	9.1963E+03	-8.8138E-01	3.2739E-05	-3.2574E-10
436	17	-9.37E-01	4.30E+01	5.6335E+02	5.1630E-01	1.2890E-04	-1.1547E-08
436	52	7.75E-01	5.26E+01	6.9704E+02	2.7727E-01	1.0047E-04	-7.4839E-09
436	764	1.17E+00	5.20E+01	9.2676E+03	-8.8859E-01	3.2898E-05	-3.2764E-10
32	764	-1.37E+01	2.09E+02	-2.9704E+04	3.8171E+00	-1.1790E-04	1.3092E-09
32	722	-1.92E+01	2.27E+02	-3.8603E+04	1.1361E+01	-8.2564E-04	2.0426E-08
32	436	-3.32E+01	1.74E+02	-3.0802E+04	3.4497E+01	-8.9643E-03	7.9935E-07
30	129	-3.94E+00	6.42E+01	-3.9698E+03	7.7278E+00	-2.4945E-03	3.0717E-07
30	59	-7.03E+00	6.29E+01	-1.9324E+03	2.5453E+00	-3.5216E-04	1.8700E-08
30	1212	-5.85E+00	6.44E+01	-4.4350E+03	4.3244E+00	-7.3584E-04	4.7308E-08
233	30	2.20E+00	4.76E+01	-1.7848E+03	1.7328E+00	-3.8315E-04	3.1888E-08
233	480	-3.29E+00	5.93E+01	1.5568E+02	5.1930E-01	-9.7529E-05	8.0431E-09
233	40	-2.62E-01	5.07E+01	2.4817E+03	-1.3841E+02	3.1134E+00	-1.9338E-02

Binary relation, cubic fit coefficients. (Page 2 of 3)

PidY	PidX	R.Mean	R.Sigma	C0	C1	C2	C3
234	30	1.03E+00	4.23E+01	-2.1335E+03	2.0427E+00	-4.7224E-04	4.0038E-08
234	480	-3.60E+00	5.30E+01	9.0938E+01	5.7480E-01	-1.1620E-04	1.0024E-08
234	40	-1.20E+00	4.19E+01	2.3131E+03	-1.2527E+02	2.7935E+00	-1.6927E-02
24	129	-5.61E+01	1.57E+03	-9.9506E+02	1.7355E+00	-4.2692E-04	5.3792E-08
24	53	-5.93E+01	1.58E+03	-2.2450E+03	3.0496E+00	-9.0553E-04	1.0751E-07
24	722	-5.50E+01	1.57E+03	-1.9156E+03	5.5106E-01	-3.2413E-05	7.9940E-10
21	93	-2.15E-02	5.52E-01	-1.2234E+02	3.1551E+00	-1.1912E-02	1.9630E-05
21	30	-8.44E-02	1.61E+00	-6.0439E+02	5.0427E-01	-1.0898E-04	7.9870E-09
21	40	1.31E-01	1.47E+00	-1.9252E+02	1.4241E+01	-1.7755E-01	7.6450E-04
176	30	-7.89E-02	1.18E+00	-2.2098E+02	1.8863E-01	-4.4176E-05	3.5617E-09
176	480	-1.48E-01	1.16E+00	-2.4065E+01	5.6079E-02	-1.3323E-05	1.1271E-09
176	129	-1.19E-01	1.14E+00	-1.2116E+02	2.0534E-01	-8.0574E-05	1.0889E-08
40	30	-8.30E-02	1.16E+00	-2.1019E+02	1.8136E-01	-4.2601E-05	3.4525E-09
40	129	-1.26E-01	1.17E+00	-1.1490E+02	1.9767E-01	-7.7579E-05	1.0519E-08
40	480	-1.55E-01	1.19E+00	-2.2246E+01	5.4551E-02	-1.2936E-05	1.0977E-09
18	225	5.98E+00	2.06E+01	4.1932E+04	-3.9638E+03	1.1780E+02	-1.1179E+00
18	1017	2.75E+01	4.50E+01	2.8680E+05	-3.0960E+04	1.0455E+03	-1.1295E+01
18	21	3.26E-01	2.01E+01	2.6417E+02	-5.0969E+00	6.5234E-02	-1.7725E-04
209	327	-7.07E+00	3.12E+01	-2.7263E+03	3.7467E+00	-1.5232E-03	2.0500E-07
209	858	-1.13E+00	2.24E+01	2.6740E+02	2.2443E+00	-2.8867E-02	1.4446E-04
209	234	1.90E+01	4.49E+01	2.9239E+03	-9.1514E+00	9.7130E-03	-3.2205E-06
93	21	5.04E-02	7.31E-01	2.5626E+02	-4.0273E+00	3.0824E-02	-5.8718E-05
93	40	2.20E-01	1.89E+00	-1.1637E+02	9.6629E+00	-8.6911E-02	2.1987E-04
93	30	-6.69E-02	1.82E+00	-5.9377E+02	5.0027E-01	-1.0822E-04	8.0011E-09
1951	990	-7.19E-02	6.12E-01	-9.5508E+00	-1.3007E-01	1.2752E-02	-1.6282E-04
1951	91	-5.40E-02	6.24E-01	3.6509E+00	-2.7187E+00	1.6642E-01	-2.8464E-03
1951	819	-4.99E-02	7.29E-01	-8.1444E+00	-3.0334E-01	9.6633E-03	1.6255E-04
90	328	-2.81E-02	1.39E+01	-2.8534E+02	1.2703E+00	-8.3125E-05	8.3040E-09
90	129	1.80E-02	1.64E+01	1.4613E+03	-7.2088E-01	7.8002E-04	-9.0049E-08
90	480	-6.14E-01	5.62E+01	-2.6407E+02	1.0769E+00	-6.6233E-05	3.6633E-09
59	480	-1.18E+00	7.31E+01	-3.2644E+02	1.6632E+00	-3.4177E-05	-2.3635E-10
59	90	-4.40E-01	7.59E+01	1.2716E+03	3.5198E-01	4.8387E-04	-4.9441E-08
59	328	-2.63E-01	7.37E+01	6.6017E+02	9.4140E-01	2.9921E-04	-3.0661E-08
659	764	-1.58E-02	1.40E+00	-1.1128E+02	1.5649E-02	-4.6284E-07	5.2739E-12
659	722	-6.15E-02	1.74E+00	-1.7074E+02	5.3144E-02	-3.7858E-06	9.3875E-11
659	52	-1.09E-01	2.08E+00	-9.8978E+01	9.5599E-02	-1.7168E-05	1.1026E-09
211	231	-6.49E+00	1.86E+01	-1.2539E+03	3.3092E+00	-2.5026E-03	6.3597E-07
211	232	-1.01E+00	1.36E+01	-7.9941E+02	2.0214E+00	-1.3739E-03	3.2295E-07
211	175	-6.72E-01	1.44E+01	-8.7893E+02	4.6998E+01	-6.7726E-01	3.3387E-03
91	990	-7.17E-02	1.00E+00	9.7311E+00	1.4153E-01	2.3244E-02	-4.8756E-04
91	1951	-3.43E-01	1.39E+00	-5.0525E+01	-3.1115E+01	-4.2091E+00	-1.7238E-01
91	211	6.57E-02	2.24E+00	-1.4748E+02	2.1704E+00	-9.2430E-03	1.2508E-05
225	1017	-4.81E-01	9.27E-01	-1.1610E+04	1.2522E+03	-4.2104E+01	4.5327E-01
225	1021	1.23E-01	3.90E-01	1.4449E+03	-1.5466E+02	5.2620E+00	-5.6936E-02
225	18	1.16E+00	8.79E-01	3.2863E+02	-3.0218E+00	9.3182E-03	-8.9316E-06
327	129	3.17E+00	8.80E+01	1.3403E+03	-9.1808E-01	8.1771E-04	-1.1088E-07
327	334	2.98E+00	8.91E+01	-1.7979E+02	8.9507E-01	-6.1215E-06	-4.3803E-09
327	480	4.26E+00	9.26E+01	9.4709E+01	5.7455E-01	2.9481E-05	-5.8128E-09
457	52	-3.43E+00	5.33E+01	-1.3671E+03	1.7357E+00	-2.0863E-04	1.4690E-08
457	436	-4.07E+00	7.00E+01	-2.0691E+03	3.0080E+00	-5.8564E-04	5.7880E-08
457	17	-8.30E+00	1.10E+02	-1.3848E+03	2.4002E+00	-4.1602E-04	4.1959E-08
650	764	-1.17E+00	3.02E+01	-5.2188E+02	6.2184E-02	-1.5675E-06	1.3148E-11
650	659	-5.72E-02	3.04E+01	-2.0071E+02	8.4735E+00	-1.4111E-02	-2.0992E-04
650	232	-2.17E+00	3.00E+01	-3.8752E+02	1.0547E+00	-6.0285E-04	1.2868E-07

.Binary relation, cubic fit coefficients. (Page 3 of 3)

PidY	PidX	R.Mean	R.Sigma	C0	C1	C2	C3
819	436	2.22E-01	4.60E+00	2.4788E+02	-1.8874E-01	5.1099E-05	-4.6515E-09
819	231	1.13E-01	5.45E+00	-4.9176E+02	1.1084E+00	-7.4935E-04	1.5923E-07
819	1951	9.51E-01	7.18E+00	-1.8709E+01	-9.9403E+00	-3.1916E-02	6.9183E-02
858	209	7.86E-01	1.92E+01	3.9170E+02	-1.6913E+00	-1.8672E-04	7.0389E-06
858	951	-6.65E+07	7.47E+08	-1.7269E+05	4.6997E+04	-5.3051E+03	4.6228E+04
858	40	1.08E+01	3.56E+01	2.4681E+03	-1.5689E+02	3.2419E+00	-2.1413E-02
951	211	-7.66E-03	7.36E+00	-2.2714E+01	3.5844E-01	-1.4698E-03	2.0190E-06
951	209	1.56E-02	7.35E+00	-1.8438E+01	2.1580E-01	-6.1634E-04	5.8292E-07
951	1951	-3.84E-02	7.39E+00	7.9617E-01	-2.1525E+00	-2.7240E-01	-1.1562E-02
990	91	1.95E-02	2.21E+00	-5.5124E+00	6.8782E-01	2.3851E-02	9.7821E-04
990	1951	-1.26E+00	3.77E+00	-1.4806E+02	-8.1164E+01	-1.1513E+01	-4.9631E-01
990	1190	-4.71E+00	1.14E+01	-6.1933E+02	2.8271E+00	-4.0396E-03	1.8606E-06
1021	225	-1.22E-01	3.07E-01	-2.4361E+03	2.3016E+02	-6.7423E+00	6.3436E-02
1021	18	-1.01E-01	1.13E+00	-2.7493E+02	2.4063E+00	-6.0037E-03	4.8780E-06
1021	231	-3.11E-01	5.41E-01	-2.0728E+02	4.9951E-01	-3.3663E-04	7.5003E-08
1017	225	7.43E-02	1.70E-01	-5.5525E+02	5.2694E+01	-1.5079E+00	1.4024E-02
1017	18	1.28E-01	3.43E-01	-7.1942E+01	6.0564E-01	-1.0323E-03	4.9995E-07
1017	231	-1.92E-01	4.38E-01	-1.5554E+02	3.7560E-01	-2.4401E-04	5.2847E-08
1058	21	-3.06E-02	7.16E-01	-6.6038E+02	1.3802E+01	-7.6796E-02	1.4222E-04
1058	93	-3.40E-02	7.20E-01	-6.2255E+02	1.2271E+01	-6.3666E-02	1.1001E-04
1058	1190	2.70E-01	1.15E+00	-4.1744E+02	1.8851E+00	-2.0287E-03	7.2605E-07
1054	21	-4.20E-02	6.98E-01	-6.7991E+02	1.4214E+01	-7.9555E-02	1.4812E-04
1054	93	-4.76E-02	7.03E-01	-6.3731E+02	1.2566E+01	-6.5545E-02	1.1383E-04
1054	1190	2.64E-01	1.14E+00	-4.2017E+02	1.8964E+00	-2.0444E-03	7.3270E-07
1188	21	-3.31E+00	3.29E+01	-7.3344E+03	1.5667E+02	-9.9426E-01	2.0732E-03
1188	1951	-1.18E+01	4.04E+01	-3.1135E+03	-1.3878E+03	-1.6064E+02	-6.0727E+00
1188	990	3.03E+00	3.33E+01	7.2107E+02	3.6779E+00	4.0670E-01	-1.6595E-02
1190	233	-1.66E+01	6.46E+01	-3.1558E+03	1.0417E+01	-9.1398E-03	2.7125E-06
1190	990	5.31E+00	6.00E+01	7.7086E+02	1.8602E+01	-4.2332E-01	1.4197E-03
1190	93	3.85E-01	5.86E+01	4.1896E+03	-8.0644E+01	5.4454E-01	-1.1173E-03
835	722	3.82E-01	6.31E+01	-1.0265E+03	4.1715E-01	-1.3988E-05	2.9807E-10
835	436	-4.19E+00	6.63E+01	1.5548E+02	4.7224E-01	1.1799E-04	-1.4230E-08
835	17	-6.31E+00	8.02E+01	7.3972E+02	-1.0329E-02	2.4156E-04	-2.4650E-08
764	659	1.46E+01	5.12E+02	5.8636E+04	-2.1189E+03	3.2695E+01	-1.3719E-01
764	17	-2.25E+01	4.76E+02	-2.6122E+04	3.5857E+01	-7.9629E-03	6.7069E-07
764	133	-1.73E+01	2.17E+02	-4.0964E+04	1.3585E+01	-9.0300E-04	2.1857E-08
175	42	6.23E-05	1.30E-01	-9.2674E+00	1.4152E+00	-6.0123E-03	2.7398E-05
175	764	-1.96E-02	9.35E-01	-2.0151E+02	2.5210E-02	-8.0957E-07	9.1205E-12
175	133	-7.45E-02	1.19E+00	-1.8009E+02	5.4913E-02	-4.0219E-06	1.0026E-10
722	371	-1.14E+01	1.09E+02	9.6896E+02	4.1943E+00	1.9786E-04	-2.4852E-08
722	764	-2.12E+00	1.01E+02	4.3345E+04	-4.3520E+00	1.6171E-04	-1.7024E-09
722	17	-1.86E+00	2.69E+02	1.2425E+04	-7.1589E+00	3.0489E-03	-2.8231E-07
1205	371	-7.90E+00	1.41E+02	4.1626E+02	4.7066E+00	-6.3951E-05	1.2976E-08
1205	17	3.35E+00	2.62E+02	1.1941E+04	-6.8474E+00	2.9289E-03	-2.6961E-07
1205	764	8.18E-01	1.11E+02	4.3395E+04	-4.3449E+00	1.6037E-04	-1.6793E-09
371	129	7.50E-01	1.64E+01	4.7155E+02	4.4346E-01	2.3809E-04	-2.8246E-08
371	722	1.99E+00	2.35E+01	1.4643E+02	1.5087E-01	4.7674E-06	-1.2077E-10
371	53	6.31E-01	2.42E+01	4.8876E+02	3.9258E-01	2.1583E-04	-2.6161E-08
328	334	3.47E-04	1.94E-04	-5.8755E-03	1.0000E+00	-1.5959E-09	1.5661E-13
328	480	-2.68E-01	2.24E+01	-4.9303E+01	9.1234E-01	-2.5353E-05	3.7728E-10
328	129	1.82E-01	2.07E+01	1.9389E+03	-1.2982E+00	1.0086E-03	-1.1966E-07
334	328	3.47E-04	1.94E-04	-5.8755E-03	1.0000E+00	-1.5959E-09	1.5661E-13
334	480	-2.68E-01	2.24E+01	-4.9303E+01	9.1234E-01	-2.5353E-05	3.7728E-10
334	12	1.82E-01	2.07E+01	1.9389E+03	-1.2982E+00	1.0086E-03	-1.1966E-07

Project Plan
for
Real-Time Sensor Data Validation

Attachment 3

Characteristic Equation Coefficients Derived in FY92 Modeling Task

```
Characteristic Relation
Fac Fuel Flow/ Lpfp Spd = constant

PID 1205 : Fac Fuel Flow
PID 32   : Lpfp Spd


Characteristic Curve Fit
#1.  PID    1205 = c1 * PID      32
#2.  PID      32 = c1 * PID    1205

-----------------------------------------
Characteristic Relation
Fac LOX Flow/ Lpop Spd = constant

PID 1212 : Fac LOX Flow
PID 30   : Lpop Spd


Characteristic Curve Fit
#3.  PID    1212 = c1 * PID      30
#4.  PID      30 = c1 * PID    1212

-----------------------------------------------
Characteristic Relation
Fac Fuel Flow/ Hpfp Spd = constant

PID 1205 : Fac Fuel Flow
PID 260  : Hpfp Spd

Characteristic Curve Fit
#5.  PID    1205 = c1 * PID     260
#6.  PID     260 = c1 * PID    1205

-------------------------------------------------------

Characteristic Relation
(Lpop Ds P - Eng Ox In P)/ (Lpop Spd)^2 = constant

PID 209  : Lpop Ds P
PID 858  : Eng Ox In P
PID 30   : Lpop Spd

Characteristic Curve Fit
#7.  PID     209 = c1 * PID     858 + c2 * PID      30^2
#8.  PID     858 = c1 * PID     209 + c2 * PID      30^2
#9.  PID      30^2 = c1 * PID     209 + c2 * PID     835
```

```
Characteristic Relation
(Hpfp In P - Eng Fuel In P)/ (Lpfp Spd)^2 = constant

PID 203  : Hpfp In P
PID 819  : Eng Fuel In P
PID 32   : Lpfp Spd

Characteristic Curve Fit
#10.  PID     203 = c1 * PID     819 + c2 * PID      32^2
#11.  PID     819 = c1 * PID     203 + c2 * PID      32^2
#12.  PID     32^2 = c1 * PID     203 + c2 * PID     819

-----------------------------------------------------

Characteristic Relation
(Hpfp Ds P - Hpfp In P)/ (Hpfp Spd)^2 = constant

PID 52   : Hpfp Ds P
PID 203  : Hpfp In P
PID 260  : Hpfp Spd

Characteristic Curve Fit
#13.  PID      52 = c1 * PID     203 + c2 * PID     260^2
#14.  PID     203 = c1 * PID      52 + c2 * PID     260^2
#15.  PID     260^2 = c1 * PID      52 + c2 * PID     203

-----------------------------------------------------

Characteristic Relation
(Hpop Ds P - Mcc Pc)/ (Fac LOX Flow)^2 = constant

PID 90   : Hpop Ds P
PID 129  : Mcc Pc
PID 1212 : Fac LOX Flow

Characteristic Curve Fit
#16.  PID      90 = c1 * PID     129 + c2 * PID    1212^2
#17.  PID     129 = c1 * PID      90 + c2 * PID    1212^2
#18.  PID    1212^2 = c1 * PID     129 + c2 * PID      90
```

```
Characteristic Relation
(Mcc Cool Ds P - Lpft In P)/ (Lpfp Spd)^2 = constant

PID 17   : Mcc Cool Ds P
PID 436  : Lpft In P
PID 32   : Lpfp Spd

Characteristic Curve Fit
#19.  PID      17 = c1 * PID     436 + c2 * PID      32^2
#20.  PID     436 = c1 * PID      17 + c2 * PID      32^2
#21.  PID      32^2 = c1 * PID      17 + c2 * PID     436

-------------------------------------------------------------

Characteristic Relation
(Hpop Ds P - Lpop Ds P)/ (Lpop Spd)^2 = constant

PID 90   : Hpop Ds P
PID 209  : Lpop Ds P
PID 30   : Lpop Spd

Characteristic Curve Fit
#22.  PID      90 = c1 * PID     209 + c2 * PID      30^2
#23.  PID     209 = c1 * PID      90 + c2 * PID      30^2
#24.  PID      30^2 = c1 * PID      90 + c2 * PID     209
```

Characteristic Curve Fit

PID 1205 = c1 * PID 32

R.Mean	R.Sigma	C1
-2.01E+04	5.34E+02	2.2997E+00

PID 32 = c1 * PID 1205

R.Mean	R.Sigma	C1
8.88E+03	2.36E+02	4.2643E-01

PID 1212 = c1 * PID 30

R.Mean	R.Sigma	C1
-3.14E+03	1.04E+02	1.7452E+00

PID 30 = c1 * PID 1212

R.Mean	R.Sigma	C1
1.82E+03	5.99E+01	5.6952E-01

PID 1205 = c1 * PID 260

R.Mean	R.Sigma	C1
-9.52E+03	1.77E+02	7.2141E-01

PID 260 = c1 * PID 1205

R.Mean	R.Sigma	C1
1.35E+04	2.42E+02	1.3679E+00

PID 209 = c1 * PID 858 + c2 * PID 30^2

R.Mean	R.Sigma	C1	C2
1.30E+02	4.65E+00	8.8237E-01	5.5824E-06

PID 858 = c1 * PID 209 + c2 * PID 30^2

R.Mean	R.Sigma	C1	C2
-1.45E+02	5.24E+00	1.1241E+00	-6.2909E-06

PID 30^2 = c1 * PID 209 + c2 * PID 835

R.Mean	R.Sigma	C1	C2
-8.11E+05	8.18E+05	-1.5730E+04	1.0035E+04

PID 203 = c1 * PID 819 + c2 * PID 32^2

R.Mean	R.Sigma	C1	C2
1.20E+02	5.99E+00	8.1231E-01	4.0383E-07

PID 819 = c1 * PID 203 + c2 * PID 32^2

R.Mean	R.Sigma	C1	C2
-8.49E+01	4.86E+00	8.2134E-01	-3.7517E-07

PID 32^2 = c1 * PID 203 + c2 * PID 819

R.Mean	R.Sigma	C1	C2
-2.29E+08	1.22E+07	2.1677E+06	-1.9919E+06

Characteristic Curve Fit

PID 52 = c1 * PID 203 + c2 * PID 260^2

R.Mean	R.Sigma	C1	C2
-1.04E+02	8.64E+01	3.8817E+00	4.3224E-06

PID 203 = c1 * PID 52 + c2 * PID 260^2

R.Mean	R.Sigma	C1	C2
1.17E+02	1.23E+01	1.1268E-01	-4.6910E-07

PID 260^2 = c1 * PID 52 + c2 * PID 203

R.Mean	R.Sigma	C1	C2
-7.46E+06	1.85E+07	2.2549E+05	-6.0593E+05

PID 90 = c1 * PID 129 + c2 * PID 1212^2

R.Mean	R.Sigma	C1	C2
-3.09E+02	1.46E+01	1.2849E+00	1.0587E-05

PID 129 = c1 * PID 90 + c2 * PID 1212^2

R.Mean	R.Sigma	C1	C2
2.97E+02	1.15E+01	7.3620E-01	-4.9742E-06

PID 1212^2 = c1 * PID 129 + c2 * PID 90

R.Mean	R.Sigma	C1	C2
-7.90E+06	5.46E+05	-2.3705E+04	2.8726E+04

PID 17 = c1 * PID 436 + c2 * PID 32^2

R.Mean	R.Sigma	C1	C2
2.57E+01	4.66E+01	1.0444E+00	-6.7441E-07

PID 436 = c1 * PID 17 + c2 * PID 32^2

R.Mean	R.Sigma	C1	C2
-4.36E+01	4.53E+01	9.3310E-01	1.1698E-06

PID 32^2 = c1 * PID 17 + c2 * PID 436

R.Mean	R.Sigma	C1	C2
4.74E+07	5.61E+06	-2.7127E+03	4.7162E+04

PID 90 = c1 * PID 209 + c2 * PID 30^2

R.Mean	R.Sigma	C1	C2
-1.10E+02	8.62E+01	9.6030E-01	1.4262E-04

PID 209 = c1 * PID 90 + c2 * PID 30^2

R.Mean	R.Sigma	C1	C2
1.68E+02	5.89E+01	6.7809E-01	-9.5686E-05

PID 30^2 = c1 * PID 90 + c2 * PID 209

R.Mean	R.Sigma	C1	C2
8.03E+05	6.04E+05	6.9911E+03	-6.5952E+03

REPORT DOCUMENTATION PAGE

Form Approved
OMB No. 0704-0188

1. AGENCY USE ONLY (Leave blank)	2. REPORT DATE	3. REPORT TYPE AND DATES COVERED
	April 1994	Final Contractor Report

4. TITLE AND SUBTITLE

Real-Time Sensor Data Validation

5. FUNDING NUMBERS

WU–584–03–11
C–NAS3–25883

6. AUTHOR(S)

Timothy W. Bickmore

7. PERFORMING ORGANIZATION NAME(S) AND ADDRESS(ES)

GenCorp
Aerojet Propulsion Division
P.O. Box 13222
Sacramento, California 95813–6000

8. PERFORMING ORGANIZATION REPORT NUMBER

E–8672

9. SPONSORING/MONITORING AGENCY NAME(S) AND ADDRESS(ES)

National Aeronautics and Space Administration
Lewis Research Center
Cleveland, Ohio 44135–3191

10. SPONSORING/MONITORING AGENCY REPORT NUMBER

NASA CR–195295

11. SUPPLEMENTARY NOTES

Technical Manager, Claudia M. Meyer, NYMA, Inc., Engineering Services Division, Brook Park, Ohio 44142. Project Manager, James W. Gauntner, Space Propulsion Technology Division, organization code 5310, NASA Lewis Research Center, (216) 433–7435.

12a. DISTRIBUTION/AVAILABILITY STATEMENT

Unclassified - Unlimited
Subject Categories 15, 16, and 20

12b. DISTRIBUTION CODE

13. ABSTRACT *(Maximum 200 words)*

This report describes the status of an on-going effort to develop software capable of detecting sensor failures on rocket engines in real time. This software could be used in a rocket engine controller to prevent the erroneous shutdown of an engine due to sensor failures which would otherwise be interpreted as engine failures by the control software. The approach taken combines analytical redundancy with Bayesian belief networks to provide a solution which has well-defined real-time characteristics and well-defined error rates. Analytical redundancy is a technique in which a sensor's value is predicted by using values from other sensors and known or empirically derived mathematical relations. A set of sensors and a set of relations among them form a network of cross-checks which can be used to periodically validate all of the sensors in the network. Bayesian belief networks provide a method of determining if each of the sensors in the network is valid, given the results of the cross-checks. This approach has been successfully demonstrated on the Technology Test Bed Engine at the NASA Marshall Space Flight Center. Current efforts are focused on extending the system to provide a validation capability for 100 sensors on the Space Shuttle Main Engine.

14. SUBJECT TERMS

Space Shuttle Main Engine; Sensors; Algorithms; Bayes Theorem; Probability theory; Mathematical models; Real-time operation

15. NUMBER OF PAGES
74

16. PRICE CODE
A04

17. SECURITY CLASSIFICATION OF REPORT	18. SECURITY CLASSIFICATION OF THIS PAGE	19. SECURITY CLASSIFICATION OF ABSTRACT	20. LIMITATION OF ABSTRACT
Unclassified	Unclassified	Unclassified	

National Aeronautics and
Space Administration

Lewis Research Center
21000 Brookpark Rd.
Cleveland, OH 44135-3191